

STUDIES IN LATE CENOZOIC VOLCANISM IN WEST - CENTRAL UTAH

I. PETROLOGY OF LATE TERTIARY
AND QUATERNARY VOLCANISM IN WESTERN
JUAB AND MILLARD COUNTIES, UTAH

C. H. Turley and W. P. Nash

II. GEOLOGY AND PETROLOGY
OF THE
FUMAROLE BUTTE VOLCANIC COMPLEX, UTAH

J. B. Peterson and W. P. Nash



UTAH GEOLOGICAL AND MINERAL SURVEY
a division of the
UTAH DEPARTMENT OF NATURAL RESOURCES

557.92
UHS
no. 52

STUDIES IN LATE CENOZOIC VOLCANISM IN WEST - CENTRAL UTAH

I. PETROLOGY OF LATE TERTIARY
AND QUATERNARY VOLCANISM IN WESTERN
JUAB AND MILLARD COUNTIES, UTAH

C. H. Turley and W. P. Nash

II. GEOLOGY AND PETROLOGY
OF THE
FUMAROLE BUTTE VOLCANIC COMPLEX, UTAH

J. B. Peterson and W. P. Nash

Property of
UTAH GEOLOGICAL & MINERAL SURVEY



UTAH GEOLOGICAL AND MINERAL SURVEY
a division of the
UTAH DEPARTMENT OF NATURAL RESOURCES

UTAH GEOLOGICAL AND MINERAL SURVEY

606 Black Hawk Way
Salt Lake City, Utah 84108

THE UTAH GEOLOGICAL AND MINERAL SURVEY is a Division of the Utah Department of Natural Resources and operates under the guidance of a Governing Board appointed by the Governor from industry and the public-at-large. The Survey is instructed by law to collect and distribute reliable information concerning the mineral resources, topography, and geology of the state, to investigate areas of geologic and topographic hazards that could affect the citizens of Utah, and to support the development of natural resources within the state. The *Utah Code Annotated, 1953 Replacement Volume 5, Chapter 36, 53-36-1 through 12*, describes the Survey and its functions.

The Survey publishes bulletins, maps, a quarterly newsletter, and a biannual journal that describe the geology of the state. Write for the latest list of publications available.

THE SAMPLE LIBRARY is maintained to preserve well cuttings, drill cores, stratigraphic sections, and other geological samples. Files of lithologic, electrical, and mechanical logs of oil and gas wells drilled in the state are also maintained. The library's collections have been obtained by voluntary donation and are open to public use, free of charge.

THE UTAH GEOLOGICAL AND MINERAL SURVEY adopts as its official policy the standard proclaimed in the Governor's Code of Fair Practices that it shall not, in recruitment, appointment, assignment, promotion, and discharge of personnel, discriminate against any individual on account of race, color, religious creed, ancestry, national origin, or sex. It expects its employees to have no interest, financial or otherwise, that is in conflict with the goals and objectives of the Survey and to obtain no personal benefit from information gained through their work as employees of the Survey. For permanent employees this restriction is lifted after a two-year absence, and for consultants the same restriction applies until publication of the data they have acquired.

TABLE OF CONTENTS

PART I VOLCANISM IN WESTERN JUAB AND MILLARD COUNTIES, UTAH
C. H. Turley and W. P. Nash

Abstract	1
Introduction.	1
Geology.	1
Honeycomb Hills.	1
Thomas Range	3
Smelter Knolls	3
Petrography	3
Rhyolite	3
Honeycomb Hills rhyolites	7
Obsidian	7
Tholeiitic Basalt	7
Basaltic Andesite.	7
Crystal Tuff and Volcanic Breccia.	7
Mineralogy	7
Feldspar	7
Biotite.	11
Topaz	11
Sphene	11
Allanite	11
Fluorite.	11
Fe-Ti Oxides.	11
Olivine	13
Orthopyroxene	13
Clinopyroxene	13
Chemistry	13
Major Elements.	13
Rhyolites.	15
Tholeiitic basalts	19
Basaltic andesite	19
Ba and Sr.	19
Rubidium	19
Geothermometry.	24
Geobarometry	24
Geothermal Resource Potential	27
Petrogenesis	29
Acknowledgment	29
Appendix.	29
A. H ₂ O Fugacity calculations	29
B. Estimation of the Free Energy for Formation of Fluortopza	30
References	31

FIGURES

Figure 1. Location map for study areas and sample sites	2
Figure 2. Geologic map of Smelter Knolls, including sample sites	5
Figure 3. Microprobe analyses of feldspars in terms of mole percent	8
Figure 4. Microprobe analyses of olivines and pyroxenes in terms of mole percent	13
Figure 5. Whole rock analyses in terms of normative quartz, albite, and orthoclase.	16
Figure 6. Selected minor and trace elements plotted against rubidium	20
Figure 7. Normalized elemental ratios obtained by dividing whole rock concentrations by those of sample MR74-3	21
Figure 8. Chondrite-normalized rare earth concentrations for rhyolites from the Honeycomb Hills	25
Figure 9. Equilibration curves between lava SK66 and the postulated mantle composition of Carmichael et al. (1977)	28

TABLES

Table 1. Paleomagnetic data	4
Table 2. Lithology key	6
Table 3. Modal analyses	6
Table 4. Average microprobe analyses of alkali feldspars	9
Table 5. Average microprobe analyses of plagioclase feldspars	10
Table 6. Average microprobe analyses of biotites.	12
Table 7. Average microprobe analyses of iron-titanium oxides	14
Table 8. Average microprobe analyses of olivines.	16
Table 9. Average microprobe analyses of pyroxenes.	17
Table 10. Chemical analyses and CIPW norms for 12 lavas and 6 residual glasses	18
Table 11. X-ray fluorescence trace element analyses	22
Table 12. Neutron activation analyses of rhyolites.	23
Table 13. Geothermometry.	26
Table 14. Geobarometry	26
Table 15. Reactions used to define the activities of components in silicate melts.	28

PART II FUMAROLE BUTTE VOLCANIC COMPLEX, UTAH

J. B. Peterson and W. P. Nash

Abstract	35
Introduction.	35
Geology.	35
Regional Geology	35
Local Geology	36
Geochronology	38
Petrography	38
Mineralogy	41
Feldspar	41
Olivine	41
Pyroxene	41
Biotite.	45
Iron - Titanium Oxides	45
Chemistry	48
Major Elements.	48
Trace Elements	48

Geothermometry	50
Petrogenesis	54
Geothermal Potential	55
Acknowledgments	55
References	55

FIGURES

Figure 1. Distribution of late Tertiary and Quaternary volcanic rocks in west-central, Utah	34
Figure 2. Geologic map of the Fumarole Butte volcanic complex	37
Figure 3. Microprobe analyses of feldspar from the Fumarole Butte Volcanic Complex.	42
Figure 4. Microprobe analyses of pyroxene (circles) and olivine (triangles) from the Fumarole Butte.	45
Figure 5. Calculated curves for equilibration of magma components (table 12)	51

TABLES

Table 1. K-Ar analytical data and ages.	39
Table 2. Paleomagnetic data	39
Table 3. Modal analyses (volume percent)	40
Table 4. Average microprobe analyses of feldspar	43
Table 5. Average microprobe analyses and structural formulas of olivines.	44
Table 6. Average microprobe analyses and structural formulas of clinopyroxenes	46
Table 7. Average microprobe analyses and structural formulas of biotites.	46
Table 8. Average microprobe analyses of iron titanium oxides	47
Table 9. Chemical analyses and CIPW norms of volcanic rocks and residual glasses.	49
Table 10. Trace element analyses (XRF values rounded to nearest 5 ppm).	51
Table 11. Reactions used to define the activities of components in silicate melts.	52
Table 12. Geothermometry.	53

STUDIES IN LATE CENOZOIC VOLCANISM IN WEST-CENTRAL UTAH

I. PETROLOGY OF LATE TERTIARY AND QUATERNARY VOLCANISM IN WESTERN JUAB AND MILLARD COUNTIES, UTAH

by C. H. Turley¹ and W. P. Nash²

ABSTRACT

The Honeycomb Hills (4.7 million years old), the Thomas Range (6.0 m.y.), and Smelter Knolls (3.4 m.y.) are three centers of relatively young rhyolitic volcanism in western Utah. Basaltic lava flows and normal faulting (which has dissected the Smelter Knolls rhyolite) are widespread in this area.

Rhyolites are both crystalline and glassy in character, with phenocrysts of quartz, alkali feldspar, oligoclase, biotite, Fe-Ti oxides, sphene, zircon, and allanite. Topaz and fluorite are found in the groundmasses of several samples. Biotites from Smelter Knolls and the Honeycomb Hills approach fluorannite in composition. Basaltic andesite and tholeiitic basalt are found at Smelter Knolls. The basaltic andesite contains plagioclase, clinopyroxene, and orthopyroxene, whereas the tholeiitic basalt has olivine in place of orthopyroxene.

Rhyolites are rich in silica, alkalis, F, Li, Be, Rb, Y, Th, U and Cl and are depleted in Al, Ca, Mg, Ti, and P. One unusual Honeycomb Hills sample contains fluorite in the groundmass, and is particularly rich in Ca and F. Chemically, the Honeycomb Hills rhyolite is the most magmatically evolved, followed by those from Smelter Knolls and the Thomas Range, respectively. Tholeiitic basalt contains 48% SiO₂, whereas the basaltic andesite is somewhat more silicic (57%).

Calculated temperatures for the rhyolites average 720°C (Thomas Range), 665°C (Smelter Knolls) and 605°C (Honeycomb Hills). Basaltic lavas crystallized at approximately 1000°C. Pressure solutions for rhyolites ranged from 20 to 1870 bars with most solutions near the low end of this range, indicating initial crystallization at shallow levels in the crust or upon extrusion.

The ages of volcanism of the rhyolite centers (6.1, 4.7 and 3.4 m. y.) suggest that none are probably

associated with a major geothermal resource. However, if the high degree of chemical evolution was caused by protracted magma residence times in the upper crust, then there may have been sizable magma bodies associated with each, and anomalously high temperatures may still be present. The large volume (>50 km³) of the Topaz Mountain rhyolite complex in the Thomas Range indicates the past presence of a large magma body. The 3.4 m.y. Smelter Knolls rhyolite system is associated with 0.3 m. y. basaltic volcanism and lies along a structural trend coincident with the Quaternary volcanism of the Crater Springs Known Geothermal Resource Area (Peterson and Nash, 1980).

INTRODUCTION

Western Juab and Millard Counties, Utah, contain numerous centers of late Tertiary volcanism which have been described by Erickson (1963), Hogg (1972), Staatz and Carr (1964) and Staub (1975). Paleozoic sediments and mid-Tertiary ignimbrites underlie most of the area. Basin and Range-type normal faulting has created several mountain ranges, some of which contain Pb-Zn, Cu-Au-Ag mineralization. Rhyolites, accompanied by ash falls, erupted 3 to 10 m.y. ago and were accompanied by basaltic flows ranging in age from 6 m.y. to less than 1 m.y. Subsequently, Pleistocene Lake Bonneville inundated the region, and lake deposits, along with alluvial fan material, have obscured low-lying outcrops.

As part of a regional geothermal resource evaluation effort, this study concentrates on the geology and petrology of the Honeycomb Hills, the Thomas Range, and Smelter Knolls, three centers of rhyolitic volcanism (figure 1).

GEOLOGY

Honeycomb Hills

The Honeycomb Hills are two domelike bodies of rhyolite with a total volume of 0.5 km³, contained within an area approximately 1.5 km in diameter. Basaltic lava flows surround the area (Hogg, 1972), and tuffs adjacent to the rhyolite contain high concentra-

¹St. Joe American Corp., Spokane, Washington

²Department of Geology and Geophysics, University of Utah, Salt Lake City, Utah 84112.

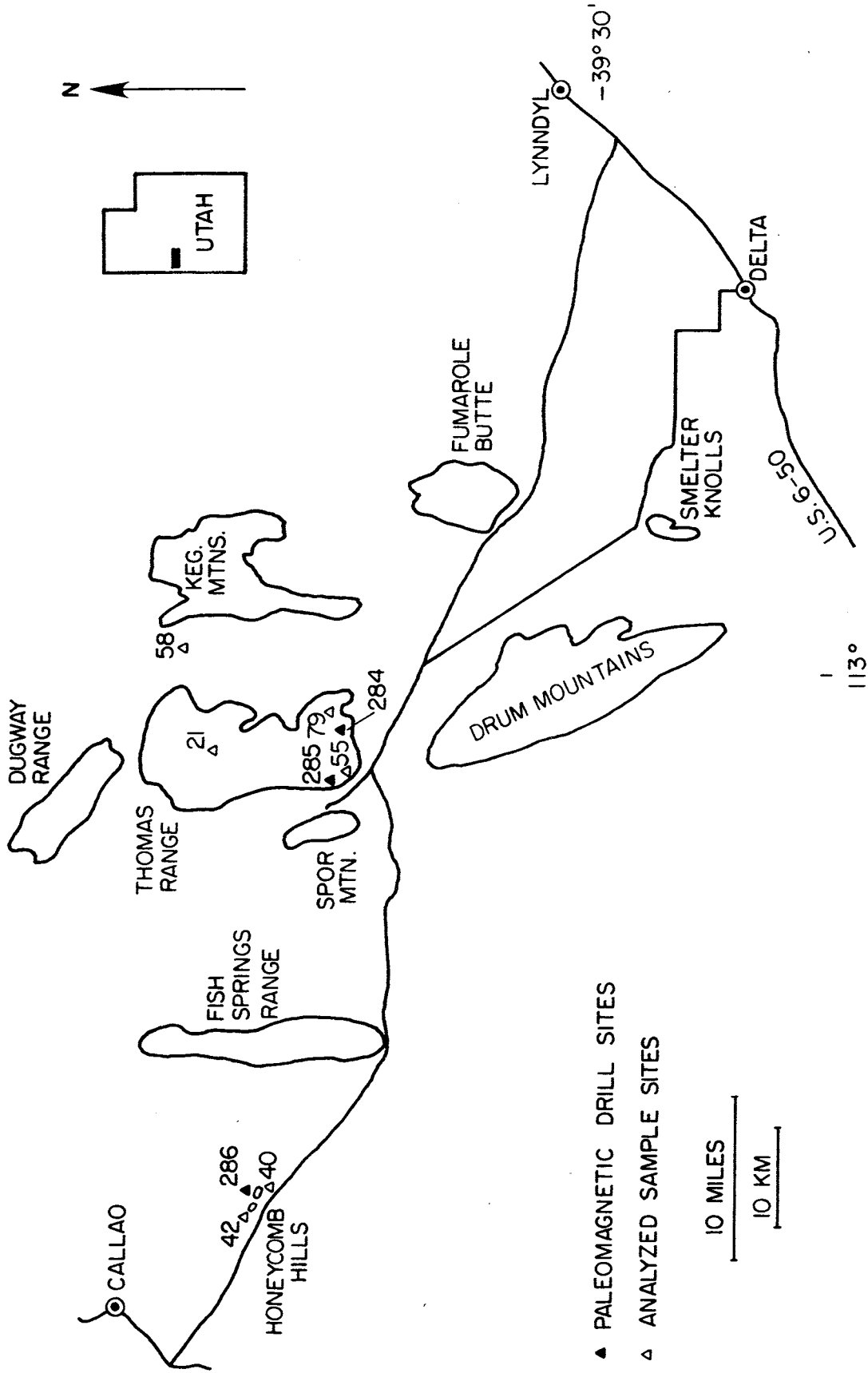


Figure 1. Location map for study areas and sample sites.

tions of Cs, Rb, Li, Be, and F (McAnulty and Levinson, 1964). The rhyolite has contorted flow layering, some of which is nearly vertical and resembles the feeder dikes described in rhyolite flows by Christiansen and Lipman (1966). Sanidine from rhyolite produced a K-Ar age of 4.65 ± 0.2 m.y. which agrees with an age of 4.7 m.y. reported by Lindsey (1977). Paleomagnetic data indicating a reversed polarity (table 1) coincides with the Gilbert reversed polarity epoch (McDougall, 1977).

Thomas Range

Staatz and Carr (1964) mapped five rhyolite flows in the Thomas Range and subdivided each of them into a basal obsidian, a thin layer of red spherulitic rhyolite, and gray rhyolite. All analyzed samples are from the obsidian and gray rhyolite units of the fifth (youngest) flow except for TR58 (figure 1, table 2), which is from an isolated outcrop of unknown age between the Thomas Range and Keg Mountains. The fifth flow has been dated at 6.0 m.y. (Armstrong, 1970), and its reversed paleomagnetic polarity suggests eruption during Epoch 6 of McDougall (1977). A notable feature of the Thomas Range rhyolite pile is its lack of structural deformation as compared to the adjacent Dugway Range and Spor Mountain, which are composed of Paleozoic sediments. The total volume of the rhyolite flows amounts to 50 km^3 , although erosion has probably removed an additional unknown amount of material.

Smelter Knolls

The Smelter Knolls are a single rhyolite flow-dome complex 5 km in diameter and 2.2 km^3 in volume (figure 2). The northern side of the main knoll has a wave-cut bench at 4800 feet elevation, the Provo level of Lake Bonneville (Hintze, 1973). Rhyolite grades irregularly from white to gray to reddish in color and it can not be differentiated into units except for scattered outcrops of basal obsidian. Dips of rhyolite flow layering tend to lessen toward the perimeter of the body, indicating a central magmatic source. However, interpretation of the flow layering is complicated by the possibility of block-flowage of the rhyolite as opposed to a totally liquid magma.

The western half of the area includes a number of isolated rhyolite bodies that have been dissected by north-south trending faults. The main, eastern knoll is 60 m higher than the western area and the two areas are divided by a normal fault 8 km in length. This fault passes near a tholeiitic basalt vent to the south and, to the north, is aligned with a fault block of a crystal tuff

probably overlain by tholeiitic basalt. Additional fault blocks of tholeiitic basalt occur from 1 to 2 km north of the knolls, and fault blocks of basaltic andesite are found 2 to 4 km to the north. Faulting in this area aligns with faults in the basaltic andesite of Fumarole Butte (Crater Springs KGRA), 12 km to the north, (Hogg, 1972; Peterson and Nash, 1980).

K-Ar dating on sanidine from rhyolite yields an age of 3.40 ± 0.1 m.y., which agrees precisely with a 3.4 m.y. date by Armstrong (1970). Rhyolite eruption near the end of the Gilbert magnetic epoch is inferred from reversed polarities at several sites.

Whole rock K-Ar dating on tholeiitic basalt from the vent south of the Knolls produced an age of 0.31 ± 0.08 m.y., and the northern basaltic andesite was dated at 6.1 ± 0.3 m.y. In contrast, tholeiitic basalt and basaltic andesite at Fumarole Butte have been dated at 6.03 ± 0.3 m.y. and $0.88 \pm .01$ m.y., respectively (Peterson and Nash, 1980), indicating at least two eruptive episodes for each mafic magma type in this area. The vent tholeiite and basaltic andesite have reversed and normal polarities, respectively, while their K-Ar ages fall in normal and reversed intervals. However, the low statistical K values for these sites may invalidate the paleomagnetic results. The normal polarity of the northern tholeiite does show that this eruption was distinct from that of the southern vent.

The crystal tuff has evidently been structurally disturbed as shown by its indefinite magnetic polarity. Caskey (1975) reports a pre-Needles Range (Oligocene) ignimbrite of normal polarity 10 km to the southwest. The Smelter Knolls tuff could well be a remnant of some cooling unit of this ignimbrite.

PETROGRAPHY

Sample numbers and lithologies are given in table 2; locations are given on figure 1. It should be emphasized that although rhyolite and obsidian denote crystalline and glassy varieties of the same rock composition, "rhyolite" is also used as a generic term to describe both.

Rhyolite

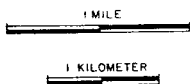
Rhyolites from Smelter Knolls and the Thomas Range are flow-banded, gray to white in color, and contain 10-20% phenocrysts (table 3). Quartz, alkali feldspar, plagioclase, biotite and Fe-Ti oxides are present in all samples. Alkali feldspar dominates over quartz in the mode, and plagioclase occurs as both twinned and

Table 1. Paleomagnetic Data

<u>Site No.</u>	<u>Site</u>	<u>Declination</u>	<u>Inclination</u>	<u>Polarity</u>	<u>No. of Samples</u>	<u>K</u>	<u>Demagnetization Intensity (Gauss)</u>
280	SK rhyolite (north)	164.4	-19.1	reversed	7	127.2	200
282	SK rhyolite (south)	170.9	-48.3	reversed	4	1250.1	200
283	SK rhyolite (southwest)	160.2	- 2.8	reversed	5	90.9	150
284	TR Topaz Valley	177.1	-50.4	reversed	5	1156.8	100
285	TR Topaz Mtn. (west)	169.7	-48.8	reversed	4	137.2	200
286	HH (central)	165.2	-53.0	reversed	7	444.5	100
312	SK vent tholeiite	155.3	- 5.6	reversed	7	11.7	100
313	SK crystal tuff	238.5	-59.4	-	3	30.3	100
314	SK north tholeiite	10.3	17.1	normal	7	13.5	--
315	SK basaltic andesite	19.6	50.7	normal	7	4.5	100

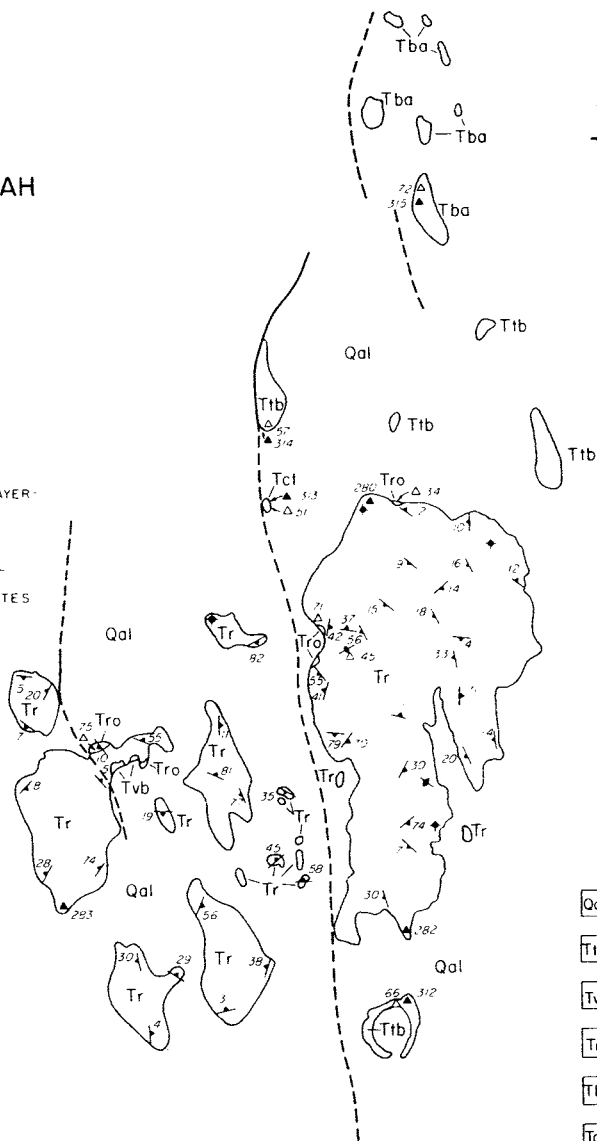
1 Paleomagnetic data were obtained from field-cored samples which were demagnetized by the alternating magnetic field method. The samples were then run a DIGICO spinner magnetometer. Variation of individual cores from their average pole position is measured by the K statistic of Fisher (1953).

GEOLOGIC MAP
OF THE
SMELTER
KNOLLS AREA
MILLARD COUNTY, UTAH

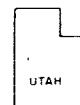


LEGEND

- CONTACT
- - - FAULT
- - - INFERRED FAULT
- 14 / ATTITUDE OF FLOW LAYERING IN RHYOLITE
- ◆ HORIZONTAL LAYERING
- ◆ VERTICAL LAYERING
- 280 ▲ PALEOMAGNETIC DRILL SITES
- 34 △ ANALYZED SAMPLE SITES



— 39°27'30"



- Qal ALLUVIUM, LAKE DEPOSITS
- Ttb THOLEIITIC BASALT
- Tvb VOLCANIC BRECCIA
- Tr, Tro RHYOLITE, OBSIDIAN
- Tba BASALTIC ANDESITE
- Tct CRYSTAL TUFF

112°52'30"

Figure 2. Geologic map of Smelter Knolls, including sample sites.

Table 2. Lithology Key

Sample	Locality	Lithology
HH40	South-central side of larger (east) Honeycomb Hill	Rhyolite
HH42	Base of Bell Hill (west Honeycomb Hill)	Rhyolite
TR21	0.7 km south of hill 6938, N. Thomas Range	Obsidian
TR55	Southwest Topaz Mountain, near paved road	Obsidian
TR58	5.5 km southeast of Bittner Knoll	Obsidian
TR79	Topaz Valley	Rhyolite
SK34	See Figure 2	Obsidian
SK45	See Figure 2	Rhyolite
SK71	See Figure 2	Obsidian
SK75	See Figure 2	Obsidian
SK57	See Figure 2	Tholeiitic basalt
SK66	See Figure 2	Tholeiitic basalt
SK72	See Figure 2	Basaltic andesite
SK51	See Figure 2	Crystal tuff

HH= Honeycomb Hills

TR= Thomas Range

SK= Smelter Knolls

Table 3. Modal Analyses (volume percent)

Sample No.	Modal Analyses (Volume Percent)											
	HH 40	SK 34	SK 45	SK 71	SK 75	TR ₂₁	TR 55	TR 58	TR 79	SK 57	SK 66	SK 72
<u>Phenocrysts</u>												
Quartz	15.8	6.4	8.6	3.7	6.3	2.8	3.4	3.8	3.8	-	-	tr.
Alkali feldspar	25.0	12.9	8.5	8.1	8.0	4.4	4.4	7.6	6.0	-	-	-
Plagioclase	0.3	0.4	0.8	0.7	0.6	0.1	0.4	0.7	0.4	24.6	45.1	7.3
Olivine	-	-	-	-	-	-	-	-	-	9.5	7.1	-
Orthopyroxene	-	-	-	-	-	-	-	-	-	-	-	1.8
Biotite	1.5	0.5	0.3	0.6	0.3	0.2	0.5	0.2	0.2	-	-	-
Fe-Ti Oxides	tr.	0.2	0.1	0.2	0.1	0.1	0.4	0.2	0.2	2.7	3.2	1.4
Sphene	-	-	-	-	-	0.1	tr.	0.3	-	-	-	-
Zircon	-	-	-	tr.	-	-	-	-	tr.	-	-	-
Topaz	0.7	-	-	-	-	-	-	-	-	-	-	-
Allanite	-	-	-	-	-	-	tr.	-	-	-	-	-
<u>Groundmass</u>												
Undifferentiated	56.7	-	81.7	-	-	-	-	-	89.4	63.2	44.6	89.5
Glass	-	79.6	-	86.7	84.7	92.3	90.9	87.2	-	-	-	-

untwinned varieties. Minor constituents include sphene, zircon, fluorite, and allanite. Topaz and hematite occur as vapor-phase products in lithophysal cavities and topaz is also present as a groundmass mineral at Smelter Knolls. Groundmasses consist of quartz and alkali feldspar along with spherulites of mixed mineralogy which have devitrified from glass.

Honeycomb Hills rhyolites contain up to 40% phenocrysts of alkali feldspar, biotite, plagioclase, and smoky-colored quartz, but Fe-Ti oxides are rare. Fluorite and acicular aggregates of topaz are abundant in the groundmass of sample HH40 (figure 1). These rocks differ from rhyolites of the other localities by having considerably larger phenocrysts and crystalline groundmasses that show no evidence of devitrification.

Obsidian

Obsidians are dark gray to black and friable because they are composed of interlocking blebs of glass; an exception is TR58, a massive obsidian. Perlitic cracks and flow-aligned crystallites are common, and phenocrysts are present in approximately the same types and proportions as in crystalline rhyolites, although fluorite and topaz were not found in obsidians.

Tholeiitic Basalt

Tholeiitic basalts are frequently vesicular with vesicle fillings of carbonate material. Groundmasses are a subophitic intergrowth of plagioclase, clinopyroxene, olivine, and Fe-Ti oxides, with interstitial residual glass. Plagioclase laths crystallized in various sizes; olivine is the only phenocryst phase.

Basaltic Andesite

Basaltic andesites have a felted groundmass of plagioclase, clinopyroxene, orthopyroxene, Fe-Ti oxides, and residual glass. Plagioclase and orthopyroxene are present as phenocrysts along with quartz. Reaction rims of orthopyroxene on the quartz indicate that the quartz was out of equilibrium with the magma under the low pressure conditions of crystallization.

Crystal Tuff and Volcanic Breccia

These lithologies are found in small outcrops at Smelter Knolls. The crystal tuff has plagioclase, biotite, amphibole, and Fe-Ti oxides in a matrix of reddish welded ash. The volcanic breccia has angular fragments of obsidian in a reddish ashy matrix similar to that of

the crystal tuff. It is associated with rhyolite and obsidian in the western knolls area, and it may represent an autobrecciated portion of the basal obsidian. However, it has been mapped as a separate unit.

MINERALOGY

Minerals in polished rock sections and from heavy liquid separates were analyzed with an ARL-EMX electron microprobe. Bence-Albee empirical corrections were made on biotites and Fe-Ti oxides, whereas other mineral analyses were corrected only for background radiation because standards similar in composition to unknowns were employed.

Feldspar

Alkali feldspar phenocrysts in rhyolites range in average composition from $Ab_{33}Or_{66}$ to $Ab_{48}Or_{51}$ (figure 3 and table 4) which is in the sanidine compositional range although some crystals have a cross-hatch twinning typical of anorthoclase. Most are not strongly zoned but are mantled near their margins. Mantling generally occurs as Ab_{50-60} edges on Ab_{35-40} cores with some rims as sodic as Ab_{68} . Groundmass sanidines evolved toward sodic (Ab_{60}) compositions in Honeycomb Hills rocks, whereas TR79 groundmass feldspars are very similar to the phenocrysts. Analysis of SK45 groundmass feldspar was complicated by abundant devitrified groundmass material.

As shown in table 5, plagioclase in rhyolites averages $Ab_{76}An_{17}$ except for Honeycomb Hills samples which average $Ab_{86}An_8$, an unusually sodic plagioclase for volcanic rocks. None of the phenocrysts are zoned, and groundmass plagioclase is not present in any of the rhyolites. Plagioclase was the initial feldspar to crystallize in several of the rhyolites, as they contain plagioclase crystals surrounded by alkali feldspar.

Tholeiitic basalt phenocrysts average $Ab_{33}An_{66}$, and many are zoned from Ab_{25} to Ab_{46} with some edges of Ab_{50-65} composition. Basaltic andesite groundmass feldspar averages $Ab_{35}An_{63}$ with zoning from Ab_{30} to Ab_{45} . Phenocrysts in this rock type are reversely zoned from An_{33} cores through a sieve-textured An_{54} portion to a thin rim of An_{69} . This reversal in zoning implies that the phenocrysts were out of equilibrium with the liquid at the time of eruption. These feldspars, along with the quartz phenocrysts, could either be remnants of cognate high pressure precipitation or pieces of crustal rock acquired during the ascent of the magma (Hausel and Nash, 1976).

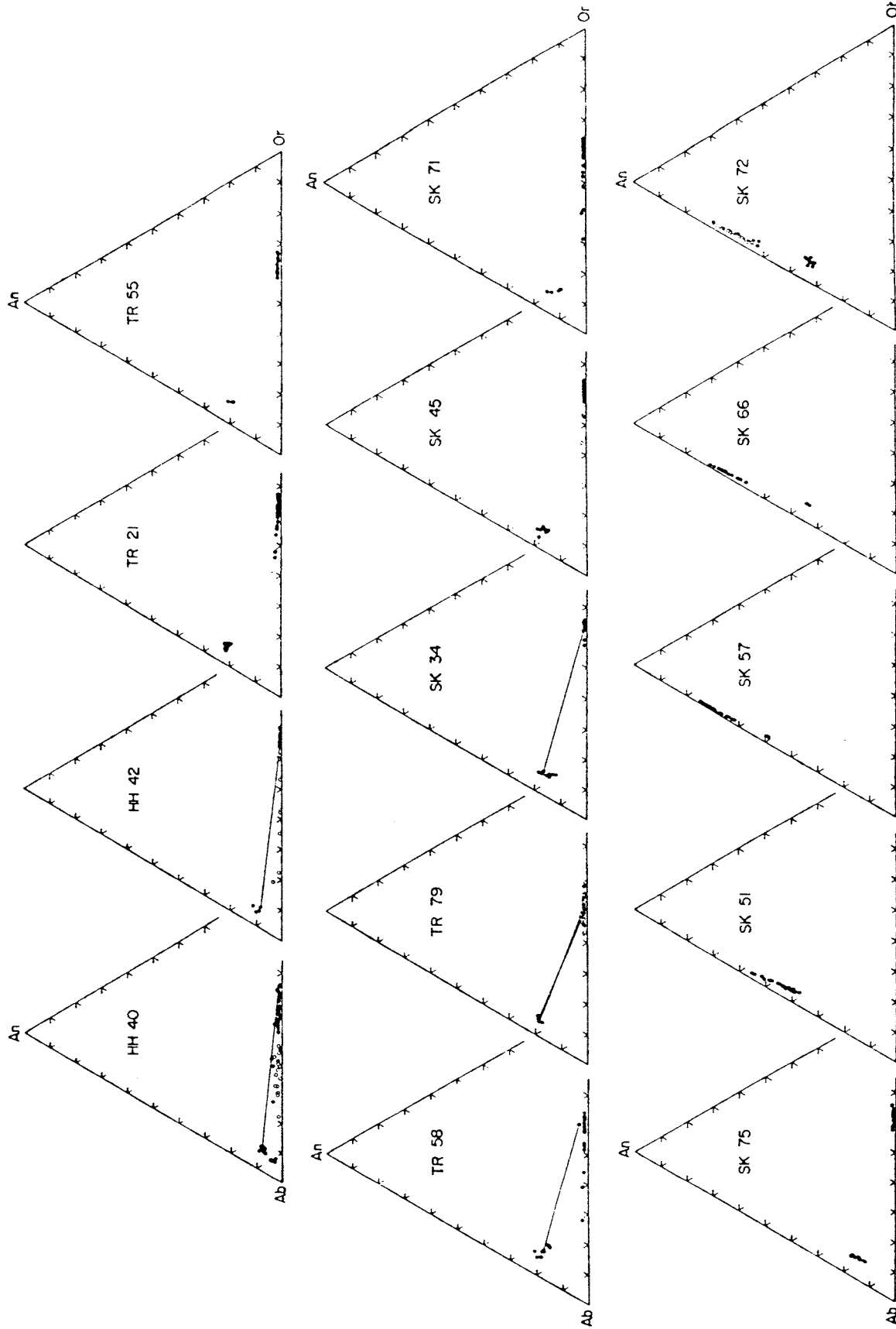


Figure 3. Microprobe analyses of feldspars in terms of mole percent anorthite (An) albite (Ab) and orthoclase (Or). Solid circles represent phenocrysts, open circles are groundmass crystals. The lines connect feldspar grains in contact with each other.

Table 4. Average Microprobe Analyses of Alkali Feldspars
 p = phenocrysts; g = groundmass

Sample No.	HH 40p	HH 40g	HH 42p	HH 42g	TR 21p	TR 55p	TR 58p	TR 79p	TR 79g	SK 34p	SK 45p	SK 45g	SK 71p	SK 75p
Weight percent														
CaO	0.31	0.86	0.09	0.22	0.28	0.27	0.36	0.29	0.33	0.21	0.21	0.26	0.21	0.19
Na ₂ O	4.76	6.84	3.76	7.26	4.11	4.02	4.73	5.40	5.54	4.08	4.28	5.78	4.56	4.23
K ₂ O	9.78	6.29	11.4	6.24	10.7	10.9	9.71	8.77	8.57	11.0	10.5	8.39	10.2	10.6
BaO	0.01	-	-	-	0.02	0.01	0.04	0.03	-	0.01	0.02	tr.	0.01	0.01
Fe ₂ O ₃ *	0.06	0.03	0.06	0.08	0.13	0.13	0.21	0.13	0.08	0.07	0.09	0.10	0.08	0.08
Weight percent														
An	1.54	4.28	0.47	1.09	1.36	1.36	1.78	1.45	1.65	1.05	1.03	1.29	1.02	0.96
Ab	40.3	57.9	31.8	61.4	34.7	34.0	40.0	45.7	46.9	34.5	36.5	48.9	38.6	36.0
Or	57.9	37.2	67.2	36.9	63.3	64.2	57.4	51.8	50.7	65.3	62.5	49.6	60.4	63.0
Cn	0.02	-	-	-	0.05	0.01	0.11	0.06	-	0.02	0.05	0.01	0.03	0.01
Total	99.7	99.4	99.5	99.4	99.4	99.6	99.3	99.0	99.3	100.9	100.1	99.8	100.1	100.0
Recalculated mole percent														
An	1.52	4.16	0.46	1.06	1.34	1.34	1.75	1.43	1.62	1.02	1.01	1.25	1.00	0.94
Ab	41.9	59.7	33.3	63.2	36.3	35.5	41.8	47.7	48.8	35.6	37.9	50.5	40.0	37.4
Or	56.6	36.1	66.3	35.7	62.3	63.2	56.5	50.9	49.6	63.4	61.1	48.3	59.0	61.7

*All iron computed as Fe₂O₃

Table 5. Average Microprobe Analyses of Plagioclase Feldspars
 p = phenocrysts; g = groundmass

Sample No.	IH 40p	IH 42p	TR 21p	TR 55p	TR 58p	TR 79p	SK 34p	SK 45p	SK 71p	SK 75p	SK 51p	SK 57p	SK 66p	SK 72p	SK 72g
Weight percent															
CaO	1.29	2.03	4.35	4.09	3.74	3.95	3.27	3.49	2.57	3.17	9.00	14.2	13.0	8.72	12.9
Na ₂ O	10.1	9.93	8.33	8.44	8.52	8.89	8.98	8.92	9.12	9.04	6.09	3.38	4.05	5.75	4.00
K ₂ O	1.23	1.00	1.16	1.31	1.58	1.00	1.32	1.21	1.48	1.29	0.60	0.15	0.28	1.31	0.38
BaO	0.01	-	0.01	-	-	0.01	0.01	tr.	-	-	0.03	0.03	0.02	0.02	0.04
Fe ₂ O ₃ *	0.07	0.04	0.28	0.24	0.41	0.19	0.17	0.17	0.12	0.13	0.33	0.70	0.84	0.31	1.04
Weight percent															
An	6.41	10.1	21.6	20.3	18.5	19.6	16.2	17.3	12.7	15.7	44.7	70.5	64.5	43.2	63.8
Ab	85.5	84.0	70.5	71.5	72.1	75.2	76.0	75.5	77.1	76.5	51.6	28.6	34.3	48.7	33.9
Or	7.28	5.89	6.87	7.74	9.35	5.93	7.80	7.17	8.72	7.62	3.57	0.88	1.63	7.74	2.23
Cn	0.03	-	0.02	-	-	0.02	0.02	0.01	-	-	0.08	0.06	0.05	0.05	0.11
Total	99.2	100.0	99.0	99.5	100.0	100.8	100.0	100.0	98.5	99.8	100.0	100.0	100.5	99.7	100.0
Recalculated mole percent															
An	6.14	9.57	20.9	19.6	17.7	18.6	15.5	16.6	12.3	15.1	43.4	69.3	62.9	42.1	62.6
Ab	86.9	84.8	72.4	73.0	73.1	75.8	77.1	76.6	79.2	77.7	53.2	29.8	35.5	50.3	35.3
Or	6.97	5.60	6.66	7.45	9.21	5.63	7.45	6.86	8.44	7.29	3.47	0.86	1.59	7.54	2.18

*All iron computed as Fe₂O₃

Crystal tuff plagioclase averages $Ab_{53}An_{43}$ and is unzoned. Sanidines are low in BaO, from 0 to 0.04%, while coexisting plagioclases have a maximum of 0.01%. BaO contents of feldspars from basaltic rocks range from 0.02 to 0.04%.

Iron contents of sanidines vary from 0.03 to 0.21% as Fe_2O_3 , and coexisting plagioclases contain 0.04 to 0.41%. Thomas Range feldspars have the highest iron contents, whereas Smelter Knolls crystals contain less Fe, and Honeycomb Hills samples are the most depleted in iron. This relation, which holds for both alkali feldspar and plagioclase, coincides with a trend of decreasing crystallization temperatures as shown by the two-feldspar geothermometer of Stormer (1975, table 12). Assuming that all iron in feldspar is present as ferric iron substituting in tetrahedral sites for aluminum, one explanation for this trend is that the $0.64A Fe^{+3}$ ion has increasing difficulty substituting for the $0.51A Al^{+3}$ ion as temperature falls. However, partitioning of iron into feldspar could also be related to oxygen fugacity (Heming, 1977), and the paucity of such data for these rocks (table 13) prevents any real resolution of this problem. Apparently Fe content in feldspars is not simply a function of whole-rock iron content. For example, Smelter Knolls feldspars contain less Fe than those from the Thomas Range, but Smelter Knolls whole-rock iron contents are up to 0.3% greater. Tholeiitic basalt plagioclases have 0.7-0.8% iron calculated as Fe_2O_3 . Basaltic andesite groundmass feldspars are rich in iron (1%), but phenocrysts contain only 0.3%.

Biotite

All crystalline rhyolites and obsidians have unzoned reddish-brown biotite phenocrysts. Thomas Range biotites, except for TR79, range from 11-17% in MgO content along with 13-21% FeO and 4.0-5.4% F (table 6). TiO_2 varies from 2.1 to 3.6% with a small amount occupying tetrahedral sites. TR79, with its low total (93%) is likely a cation-deficient biotite with considerable ferric iron in octahedral sites. Foster (1964) notes a positive correlation between Li and F in micas. Considering that the biotites from these rhyolites are fluorine-rich, they could also contain octahedral lithium, which, unfortunately, cannot be analyzed with the microprobe.

In contrast, Smelter Knolls and Honeycomb Hills biotite phenocrysts contain only 0.3-5.1% MgO with 27.5-36.2% iron as FeO and 2.3-5.7% F. These compositions, approaching fluorannites, are highly unusual in light of experimental results obtained by Munoz and Ludington (1974), who argue that the affinity between

Mg and F in biotites is much stronger than that between Fe and F. Smelter Knolls biotites have 2.3-3.7% TiO_2 and relatively high Cl (0.4%). SK45 (rhyolite) biotite has significantly more Mg and F than crystals from obsidians of that area. Honeycomb Hills biotites are very low in TiO_2 and are high in Al_2O_3 (17-18%), with Al^{+3} serving as a significant octahedral site constituent. HH40 phenocrysts are also high in MnO and CaO. SK51 (crystal tuff) biotite as 15% MgO, 15% FeO, and 1.0% F.

Topaz

Topaz is a ubiquitous lithophysal crystal and is also found in the groundmasses of Honeycomb Hills and Smelter Knolls rhyolites. Groundmass topaz crystals from HH40, HH42, and SK45 were analyzed for fluorine and respectively contain 19.6, 19.9, and 20.1% F. Penfield and Minor (1894) reported 20.3% F in Thomas Range topaz, compared to a maximum of 20.65% F for stoichiometric fluorotopaz.

Sphene

Sphene is common in Thomas Range rocks, but it was not found in the other areas. Sphenes from TR58, TR55, and TR21 were analyzed for fluorine and contain 0.7, 0.8 and 0.6% respectively.

Allanite

Allanite, an epidote group mineral rich in rare-earth elements, was identified in TR55, but was not analyzed. Evans (1978) has analyzed allanite in Quaternary rhyolites from the Mineral Range, Utah.

Fluorite

Fluorite is abundant in HH40 and is found in small amounts in TR79, SK45, and HH42. HH40 fluorite has 0.10% Sr, while strontium is below the limit of detection (0.03%) in the other fluorites. The reason for this difference is strontium content is not clear, although Yakubovich and Portnov (1967) report that the Sr content of post-magmatic fluorite related to alkalic rocks is approximately two orders of magnitude greater than the amount of strontium in fluorite related to granitic rocks.

Fe-Ti Oxides

Homogenous coexisting iron-titanium oxides were found in only three samples (table 7). Titanomagnetite is present in all rock types, but ilmenite is extremely rare

in rhyolites. This rarity is probably due to low TiO_2 content, although Haggerty (1976) discusses "sphenitization", an alteration process in which ilmenite is selectively replaced by sphene. Several rocks have sphene crystals surrounding Fe-Ti oxides, so this process may be controlling the abundance of ilmenite.

Thomas Range titanomagnetite has more Mn and Mg along with less Ti and Cr than the Smelter Knolls counterpart. Analyses of three samples from each area averaged 0.01% Cr_2O_3 in the Thomas Range crystals and 0.04% at Smelter Knolls. This is the only instance in which rhyolites from Smelter Knolls appear less evolved than those of the Thomas Range.

Olivine

Olivine occurs as phenocrysts and groundmass crystals in tholeiites (table 8). SK57 phenocrysts are most strongly zoned near the edges with rims of composition Fa_{24-28} on Fa_{20-24} cores (figure 4). Some olivines from SK66 are progressively zoned from Fa_{30} to Fa_{46} . Relative to phenocrysts, groundmass olivines in both samples are enriched in Fe and Mn and depleted in Ni.

Orthopyroxene

Basaltic andesite contains groundmass crystals and unzoned phenocrysts of orthopyroxene (table 9). Groundmass crystals are enriched in Ti, Fe, Mn, and Ca and depleted in Al and Mg relative to phenocrysts. In figure 4 several SK 72 analyses fall within the solvus field between clinopyroxene and orthopyroxene. These may be metastable compositions, or they could be caused by simultaneous analysis of different pyroxene grains by the microprobe beam.

Clinopyroxene

Groundmass grains of augitic clinopyroxene are found in both tholeiitic and basaltic andesite. SK72 augites are enriched in Na and Ti as compared to coexisting orthopyroxenes. The higher silica content of augite from basaltic andesite reflects its higher whole-rock silica content relative to tholeiitic basalt, a relationship noted by Wender and Nash (1979).

CHEMISTRY

Major Elements

Whole rock analyses were performed by wet

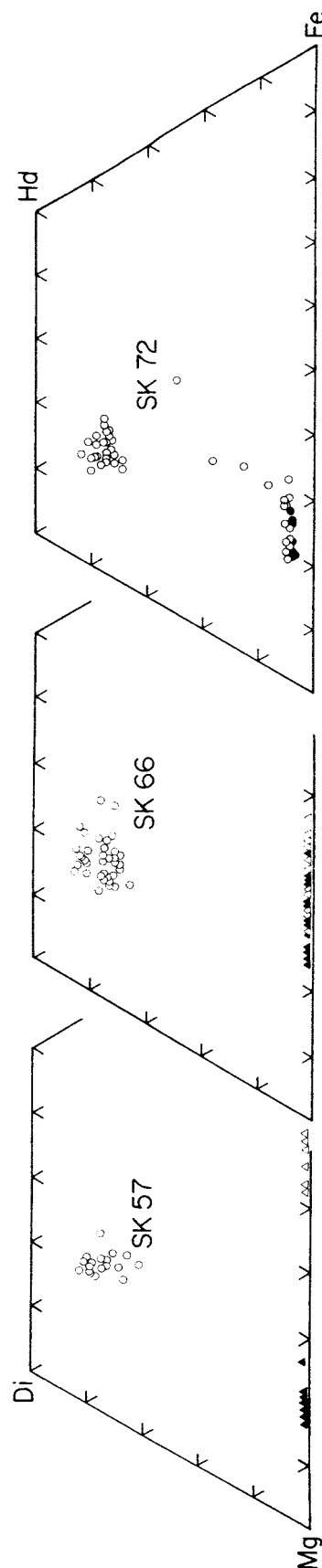
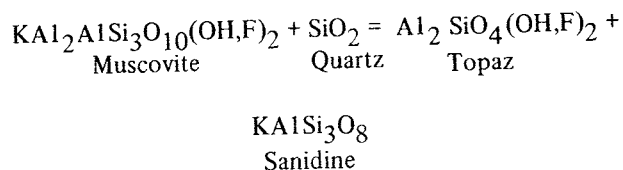


Figure 4. Microprobe analyses of olivines and pyroxenes in terms of mole percent diopside (Di) hedenbergite (Hd) and Mg and Fe-rich end members representing forsterite and fayalite for olivines and enstatite and ferrosillite for pyroxenes. Triangles indicate olivines, circles are phenocrysts; open symbols are groundmass compositions.

chemical procedures described by Carmichael et al. (1968); in addition, fluorine was determined colorimetrically by the lanthanum alizarine blue method. Analyses are given in table 10. Rhyolites and obsidians are rich in silica (74.8-77.2%, on an anhydrous basis), total alkalis (8-9%) and fluorine (0.2-8.0%). Al, Ca, Mg, Ti, and P contents are low, while Ca:Mg and Fe:Mg ratios are high. Whole rock compositions in terms of normative albite-orthoclase-quartz are shown in figure 5. All samples fall near the minimum melting composition for this system (Tuttle and Bowen, 1958).

Rhyolites usually contain normative corundum. This is due in part to normative fluorite which consumes calcium in the calculation so that no normative anorthite is formed, thus leaving an excess of Al_2O_3 . On the other hand, the presence of topaz may indicate a truly peraluminous melt. Carmichael et al. (1974) doubt the existence of peraluminous acid magmas because of the rarity of andalusite and garnet rhyolites. Perhaps topaz-bearing rhyolites, which are found in several areas in the western United States, fill this petrologic category. Muscovite does not occur in volcanic rocks, and the solid-solid reaction:



suggests that topaz, rather than muscovite, crystallizes in fluorine-rich, peraluminous rocks under low-pressure conditions. Calculation of molar volumes for these phases yields a molar volume change of $+0.59 \text{ cm}^3$ for the reaction as written, indicating that topaz crystallization is favored by lower pressures.

Wyllie and Tuttle (1961) note that high HF and Li_2O contents in granitic melts lower the solidus temperature for the system and also promote the growth of large albite crystals. Lithium contents of these rhyolites are not excessively large (200 ppm), but their HF concentrations were high, as shown by high whole-rock fluorine contents, particularly at the Honeycomb Hills. Thus, the relatively large feldspar phenocrysts in Honeycomb Hills rhyolites could be a result of high HF content of the melt.

HF can also affect the order of crystallization of minerals in granitic melts (von Platen and Winkler, 1961; von Platen, 1965). At a vapor pressure of 2000 b, hy-

drous granitic melts crystallize from 710 to 676°C in the order magnetite-biotite-K-feldspar-quartz-plagioclase. When HF is added to the melt, the crystallization interval drops to 663-640°C, and the order becomes quartz-plagioclase-biotite-K-feldspar. Therefore, fluorine may alter the two-feldspar phase relationships and cause mantling of plagioclase by alkali feldspar. Glyuk and Anfilogov (1973) argue that the reaction of plagioclase with HF in a melt can produce such minerals as topaz and fluorite, a process which may account for the unusual mineral assemblage in HH40.

Smelter Knolls rhyolites have a higher Na:K ratio than those from the Thomas Range, along with more Al and Fe and less Ti and Mg. SK45 is diopside-normative because of its high CaO content which reflects the presence of fluorite and secondary calcite. Its fluorine content is considerably lower than cogenetic obsidians, evidence that fluorine is lost during devitrification. SK71 and SK75, although areally separated by 2 km, are remarkably similar in whole rock and mineral chemistry, which supports the conclusion that the Smelter Knolls are derived from a single magma body.

The single Honeycomb Hills rhyolite which was analyzed is very unusual. HH40 contains 11.08% CaO, 7.97% F, and only 63.51% SiO_2 . This strange composition is due to the large amount of groundmass fluorite, calculated as 15.3% in the norm. When this rock is plotted in the granite system ternary (figure 5), it falls only slightly below the other samples, demonstrating that its average composition (minus fluorite) is close to a rhyolite. Its low analytical total (98.89%) may be caused by fluorine interference with silica analysis, although silica determinations were made with three methods: the classical sodium carbonate fusion method, the high-fluorine (ZnO) method of Shell and Craig (1954), and the metaborate fusion procedure of Shapiro (1975) which yielded the highest value (63.51%). Low silica would account for its location in the granite system being slightly farther displaced from the quartz apex as compared to the other samples. HH40 also has very low TiO_2 and MgO contents along with more P_2O_5 and slightly less Al_2O_3 than the other rhyolites.

Shawe (1966) reports a Honeycomb Hills rhyolite with 74% SiO_2 , 1.5% CaO and 0.79%F. Four additional samples were analyzed for fluorine, and these yielded 0.65, 0.78, 0.79, and 1.08% F; HH40 is anomalous. However, there is no field evidence that it is from a dike or any other such late-stage feature; its outcrop is similar in appearance to the rest of the rhyolite body. It apparently represents a local accumulation of fluorine

Table 8. Average Microprobe Analyses of Olivines

Average microprobe analyses of olivines
p = phenocrysts; g = groundmass

Sample No.	SK 57p	SK 57g	SK 66p	SK 66g
SiO ₂	38.6	33.5	38.0	35.8
FeO*	17.1	45.5	24.9	32.0
MnO	0.26	0.60	0.30	0.50
MgO	42.7	19.8	36.3	31.0
CaO	0.54	0.55	0.55	0.59
NiO	<u>0.17</u>	<u>0.12</u>	<u>0.15</u>	<u>0.08</u>
TOTAL	99.4	100.1	100.2	100.0
Fo	74.5	34.6	63.4	54.0
Fa	24.3	64.6	35.4	45.3
La	0.84	0.84	0.85	0.91
Tp	0.37	0.85	0.43	0.71
Ni-01	<u>0.24</u>	<u>0.17</u>	<u>0.21</u>	<u>0.11</u>
TOTAL	100.3	101.1	100.3	101.0

Recalculated mole percent

Fo	74.8	43.3	63.6	62.8
Fa	24.4	55.8	35.5	36.4
La	0.84	0.87	0.85	0.85

*All iron computed as FeO

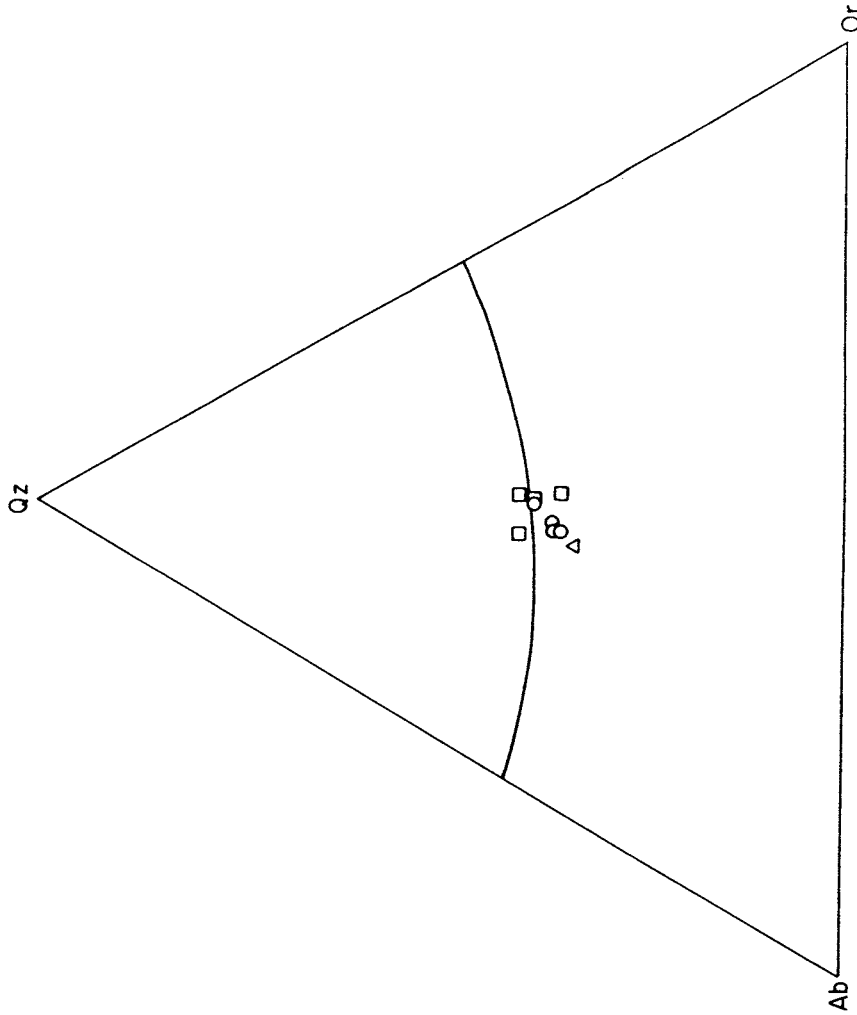


Figure 5. Whole rock analyses in terms of normative quartz, albite, and orthoclase. Squares, circles, and triangles represent Thomas Range, Smelter Knolls, and Honeycomb Hills samples, respectively. The curved quartz-feldspar field boundary is drawn at 1 Kbar water pressure.

Table 9. Average Microprobe Analyses of Pyroxenes
p = phenocrysts; g = groundmass

Sample No.	<u>Clinopyroxenes</u>			<u>Orthopyroxenes</u>	
	SK 57g	SK 66g	SK 72g	SK 72g	SK 72p
SiO ₂	48.1	50.1	53.4	53.8	52.8
TiO ₂	1.58	1.16	0.43	0.10	-
Al ₂ O ₃	3.14	2.39	2.26	1.53	2.17
FeO*	14.3	13.1	12.0	15.6	13.9
MnO	0.30	0.32	0.37	0.42	0.29
MgO	13.6	14.5	15.0	25.1	27.8
CaO	18.5	18.7	17.9	2.71	1.89
Na ₂ O	0.30	0.35	0.28	0.07	0.07
TOTAL	99.8	100.6	101.6	99.3	98.9
<u>Recalc. Mole %</u>					
En	39.0	41.1	43.4	70.1	75.2
Fs	23.0	20.9	19.4	24.4	21.1
Wo	38.0	38.0	37.2	5.5	3.7
<u>Number of ions on the basis of 6 oxygens</u>					
Sample No.	SK 57g cpx	SK 66g cpx	SK 72g cpx	SK 72g opx	SK 72p opx
Si	1.84	1.89	1.96	1.97	1.92
Al	0.14	0.11	0.04	0.03	0.08
Ti	0.02	-	-	-	-
Al	-	-	-	0.04	0.01
Ti	0.03	0.04	0.01	tr.	-
Fe ⁺²	0.46	0.41	0.37	0.48	0.42
Mn	0.01	0.01	0.01	0.01	0.01
Mg	0.78	0.81	0.82	1.37	1.51
Ca	0.76	0.75	0.70	0.11	0.07
Na	0.02	0.02	0.02	0.01	0.01

*All iron computed as FeO

Table 10. Chemical Analyses and CIPW Norms for 12 Lavas and 6 Residual Glasses

Sample No.	SK 72	SK 57	SK 66	SK 34	SK 45	SK 71	SK 75	TR 21	TR 55	TR 58	TR 79	HH 40	SK 34G	SK 71G	SK 75G	TR 21G	TR 56	TR 58G
SiO ₂	57.33	47.96	47.88	74.51	76.22	73.55	74.61	74.70	72.17	74.73	76.69	63.51	73.3	74.0	75.2	75.7	76.2	74.8
TiO ₂	1.08	1.68	2.05	0.03	0.04	0.03	0.05	0.13	0.13	0.21	0.19	tr.	0.06	0.03	0.04	0.11	0.10	0.14
Al ₂ O ₃	15.55	15.09	14.85	12.37	11.84	12.74	12.54	12.20	11.99	11.85	12.03	11.04	12.5	12.9	12.8	12.2	12.1	11.6
Fe ₂ O ₃	3.07	2.95	2.15	0.03	0.17	0.22	0.05	0.19	0.64	0.18	0.84	0.25	n.d.	n.d.	n.d.	n.d.	n.d.	n.d.
FeO*	4.06	7.60	9.36	1.04	1.03	0.85	1.00	0.69	0.34	0.65	0.10	0.43	0.73	0.44	0.40	0.28	0.39	0.47
MnO	0.14	0.17	0.16	0.04	0.04	0.03	0.04	0.04	0.04	0.04	0.04	0.03	0.05	0.03	0.05	0.04	0.04	0.05
MgO	3.99	8.48	7.45	0.03	0.08	0.11	0.10	0.08	0.08	0.08	0.09	0.05	0.02	0.01	0.01	0.02	0.02	0.02
CaO	6.94	11.25	10.22	0.52	1.86	0.80	0.64	0.84	2.65	0.71	0.74	11.08	0.36	0.32	0.23	0.44	0.32	0.46
Na ₂ O	3.19	2.31	2.87	3.73	3.45	3.89	3.85	3.52	3.27	3.58	3.26	3.63	3.65	3.64	3.31	3.48	3.40	3.60
K ₂ O	2.55	0.45	0.81	4.76	4.77	4.65	4.61	5.40	4.75	4.17	5.03	3.99	4.72	4.90	5.14	5.16	5.45	4.09
P ₂ O ₅	0.47	0.33	0.44	0.00	0.01	0.00	0.00	0.00	0.00	0.00	0.00	0.03	n.d.	n.d.	n.d.	n.d.	n.d.	n.d.
CO ₂	0.30	0.58	0.81	0.04	0.44	0.04	0.06	0.26	1.92	0.06	0.03	0.10	n.d.	n.d.	n.d.	n.d.	n.d.	n.d.
F	n.d.	n.d.	n.d.	0.65	0.45	0.78	0.71	0.23	0.21	0.14	0.23	7.97	0.49	0.65	0.84	0.12	0.16	0.09
H ₂ O ⁺	0.60	0.40	0.43	1.80	0.00	1.89	1.50	1.36	1.31	2.98	0.47	0.10	n.d.	n.d.	n.d.	n.d.	n.d.	n.d.
H ₂ O ⁻	0.13	0.13	0.24	0.16	0.13	0.19	0.34	0.12	0.25	0.19	0.04	0.04	n.d.	n.d.	n.d.	n.d.	n.d.	n.d.
Sum	99.40	99.38	99.72	99.71	100.53	99.77	100.10	99.76	99.75	99.57	99.78	102.25	95.9	96.9	98.0	97.6	98.2	95.3
-0.3F	-	-	-	0.27	0.19	0.33	0.30	0.10	0.09	0.06	0.10	3.36	0.21	0.27	0.35	0.05	0.07	0.04
Total	99.40	99.38	99.72	99.44	100.34	99.44	99.80	99.66	99.66	99.51	99.68	98.89	95.7	96.6	97.7	97.5	98.1	95.3
CIPW Norms																		
q	10.71	-	-	33.68	35.72	32.33	33.61	32.63	34.85	36.56	37.56	26.76	33.36	33.69	35.91	34.93	35.07	37.14
c	-	-	-	1.08	-	1.31	1.22	0.26	1.47	0.67	0.56	0.75	1.39	1.61	1.79	0.41	0.46	0.66
or	15.07	2.66	4.79	28.13	28.19	27.48	27.24	31.91	28.07	24.64	29.72	23.58	27.89	28.96	30.37	30.49	32.21	24.17
ab	26.99	19.55	24.28	31.56	29.19	32.92	32.58	29.79	27.67	30.29	27.59	30.72	30.89	30.80	28.01	29.45	28.77	30.46
an	20.58	29.48	25.25	-	2.73	-	-	0.84	-	2.12	1.80	-	-	-	-	1.30	0.42	1.62
di-wo	3.71	8.56	7.29	-	0.15	-	-	-	-	-	-	-	-	-	-	-	-	-
di-en	2.54	5.58	4.19	-	0.02	-	-	-	-	-	-	-	-	-	-	-	-	-
di-fs	0.87	2.39	2.78	-	0.15	-	-	-	-	-	-	-	-	-	-	-	-	-
en	7.39	12.69	7.02	0.07	0.18	0.27	0.25	0.20	0.20	0.20	0.22	0.12	0.05	0.02	0.02	0.05	0.05	0.05
fs	2.53	5.45	4.66	1.91	1.61	1.39	1.79	0.97	-	0.77	-	0.64	1.33	0.81	0.76	0.41	0.63	0.72
fo	-	1.99	5.15	-	-	-	-	-	-	-	-	-	-	-	-	-	-	-
fa	-	0.94	3.77	-	-	-	-	-	-	-	-	-	-	-	-	-	-	-
mt	4.45	4.28	3.12	0.04	0.25	0.32	0.07	0.28	0.85	0.26	-	0.36	-	-	-	-	-	-
il	2.05	3.19	3.89	0.06	0.08	0.06	0.09	0.25	0.25	0.40	0.30	-	0.11	0.06	0.08	0.21	0.19	0.27
hm	-	-	-	-	-	-	-	-	0.05	-	0.84	-	-	-	-	-	-	-
ap	1.11	0.78	1.04	-	0.02	-	-	-	-	-	-	0.07	-	-	-	-	-	-
fr	-	-	-	0.72	0.92	1.11	0.89	0.47	0.43	0.29	0.47	15.37	0.50	0.45	0.32	0.25	0.33	0.18
cc	0.68	1.32	1.84	-	1.00	-	-	0.59	4.18	0.14	0.07	-	-	-	-	-	-	-
rest	0.73	0.53	0.67	1.96	0.13	2.08	1.84	1.48	1.56	3.17	0.51	0.14	-	-	-	-	-	-
Total	99.42	99.40	99.74	99.22	100.34	99.26	99.58	99.66	99.57	99.51	99.68	98.51	95.53	96.39	97.27	97.50	98.11	95.28

*All iron in glasses computed as FeO

Analysts: C. H. Turley, J. B. Petersen and W. P. Nash.

in the crystallizing mass.

In terms of its chemical composition, HH40 with only 63% silica cannot be considered a true rhyolite. Orgonites, described by Kovalenko et al. (1971), are topaz-bearing quartz keratophyre dike rocks with 70-71% SiO₂, 8-9% total alkalis, and 1.3-2.6% F. These rocks are some of the most similar to HH40 that have been reported in the literature; nevertheless they do not approach its high concentrations of calcium and fluorine. High calcium in such a highly evolved rock is unusual because Ca is commonly removed early in magmatic processes. Apparently fluorine in melts tends to coordinate with calcium (Kogarko and Krigman, 1966), which may account for the frequent association of fluorite with granitic rocks.

Residual glasses were analyzed with the microprobe, and low analytical totals reflect their high water content. They are depleted in Ti, Mg, and F relative to whole rock analyses as these elements partition into phenocrysts such as Fe-Ti oxides and biotite.

Tholeiitic basalts contain 48% SiO₂, 15% Al₂O₃, and less than 3% total alkalis. They are olivine and hypersthene-normative, which qualifies them as olivine tholeiites, characterized by Best and Brimhall (1974) as a transitional variety between alkali-olivine and tholeiitic basalts in the western United States. The whole-rock alkali content cannot be accounted for by feldspars, which indicates that the interstitial glass must be alkali-rich. The small size of individual particles of the glass prevented microprobe analysis.

Basaltic andesite is quartz-normative (57% SiO₂) and is similar to the quartz-bearing basaltic andesites of northern Arizona and southern Utah (Best and Brimhall, 1974). Ti, Fe, Mg, and Ca are lower than in the tholeiites, and alkalis are higher.

Trace element concentrations were determined for twenty-nine elements (table 11), with Li, Be, U, and Cl determined only in silicic samples. Li and Be were analyzed by atomic absorption spectroscopy, and all other elements were determined by X-ray fluorescence or neutron activation.

Ba and Sr are high in the tholeiites (SK56, 66) and in the basaltic andesite (SK72). Nb similarly increases fivefold, and Zr more than doubles. Pb and Th are very low in the basaltic rocks. Zn is fairly constant (40-60 ppm) in all rock types except for the Honeycomb Hills rhyolites, which have only 20 ppm.

Rubidium has an extremely high liquid/crystal partition coefficient for most igneous processes. It is taken as an index of degree of evolution for these rocks. When plotted against Rb (figure 6), seven minor and trace elements in rhyolites show definite trends. Values from rhyolites of Utah's Mineral Range (Evans, 1978), have been added for comparison. Normally, Y, F, and Li increase with Rb content whereas Ba, Sr, Zr, and Ti decrease. Thomas Range rhyolites exhibit some anomalous behavior with higher Ti and Zr and lower F and Li as compared to the general trends. Smelter Knolls rocks have moderately high Zr and unusually high Y (125-185 ppm). The strontium trend is not adhered to by HH40, which has 200 ppm. Most of this Sr is incorporated into fluorite because the 0.10% (1,000 ppm) strontium content multiplied by 15.37% normative fluorite accounts for 154 ppm whole-rock Sr. Li ranges up to 201 ppm in HH40, and some Smelter Knolls samples have nearly 150 ppm.

Elemental concentrations were normalized to sample MR 74-3 of Evans (1978), an extensively analyzed rhyolite from the Mineral Range which is one of the least evolved Quaternary rhyolites from that area (figure 7). On this basis, the Juab-Millard rhyolites are comparatively enriched in Li, Be, F, Rb, Y, Nb, Th, and U, and are depleted in Sr (except for HH40) and Ba. Major element ratios show little significant variation.

Beryllium, with the exception of TR58 (7 ppm) is fairly constant in all samples at 10-14 ppm and shows no preference for obsidians over rhyolites. Beryllium left over from magmatic processes may be responsible for the Be mineralization adjacent to the Thomas Range and Honeycomb Hills (Shawe, 1966). Nb, Pb, and Th contents are roughly equal in all rhyolites. Uranium is a consistent 10-15 ppm at the Thomas Range and Smelter Knolls, but HH42 (a "normal" Honeycomb Hills rhyolite with 0.79% F) has 20 ppm and HH40 contains an extreme 150 ppm. Chlorine values range from 0-265 ppm in rhyolites to 520-970 ppm in obsidians, indicating that Cl, along with F is lost during devitrification. This effect has been noted in several other studies (Noble et al., 1967; Lipman et al., 1969; Rosholt et al., 1971; Zielinski et al., 1977). Smelter Knolls rocks are the most chlorine-rich of the three areas.

Results of neutron activation analyses are presented in table 12. Values for U and Th confirm the XRF data. HH40 has anomalously high U content. A more representative rhyolite from Honeycomb Hills, HH42, has 16.7 ppm U. Rb values are similar by NAA and XRF methods except for HH40 and SK75. We have

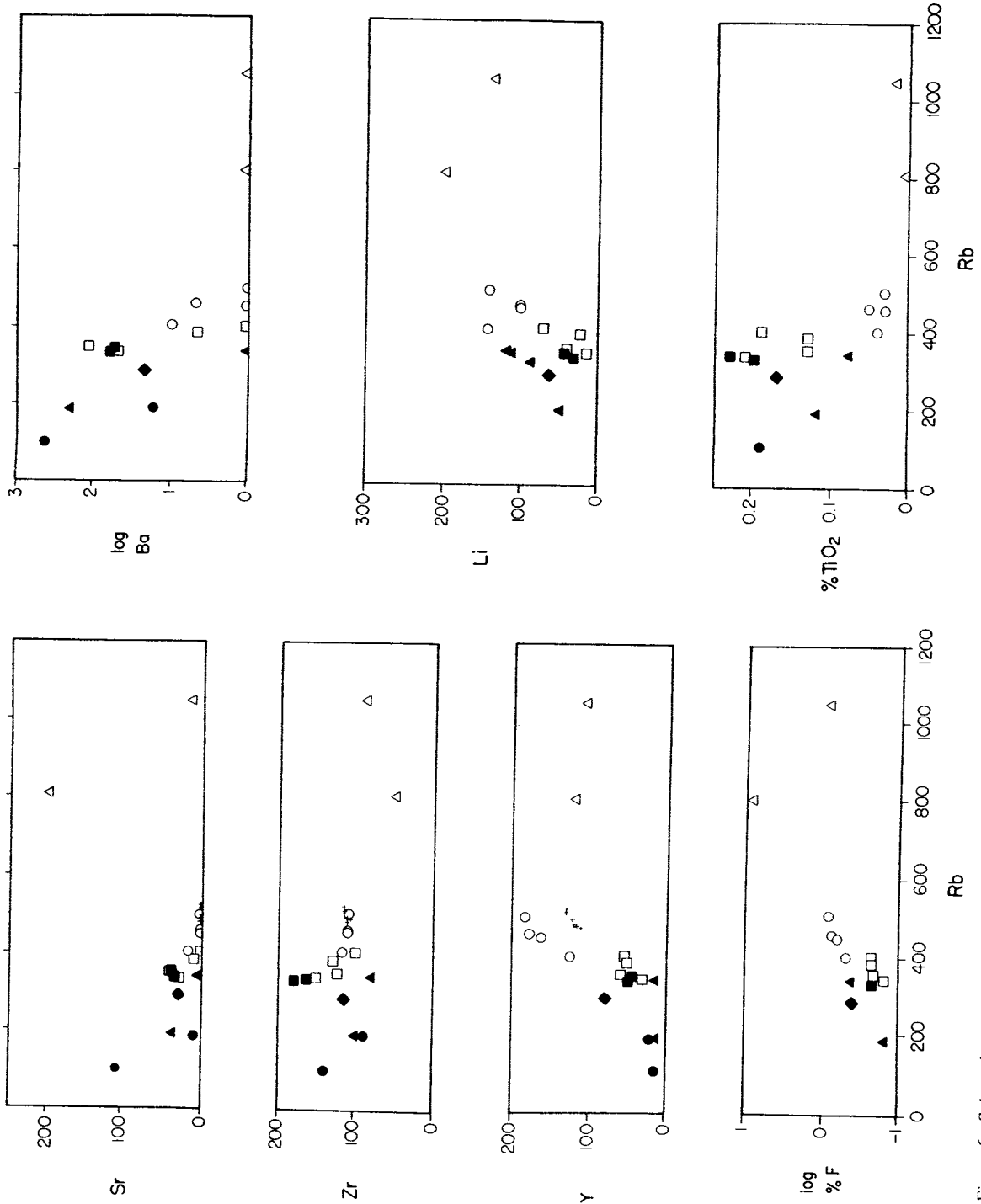


Figure 6. Selected minor and trace elements plotted against rubidium. Values are in ppm unless noted. Various symbols represent samples from the following areas: solid triangles - Mineral Range, Utah (Evans and Nash, in press); open squares - Thomas Range; open circles - Smetter Knolls; open triangles - Honeycomb Hills.

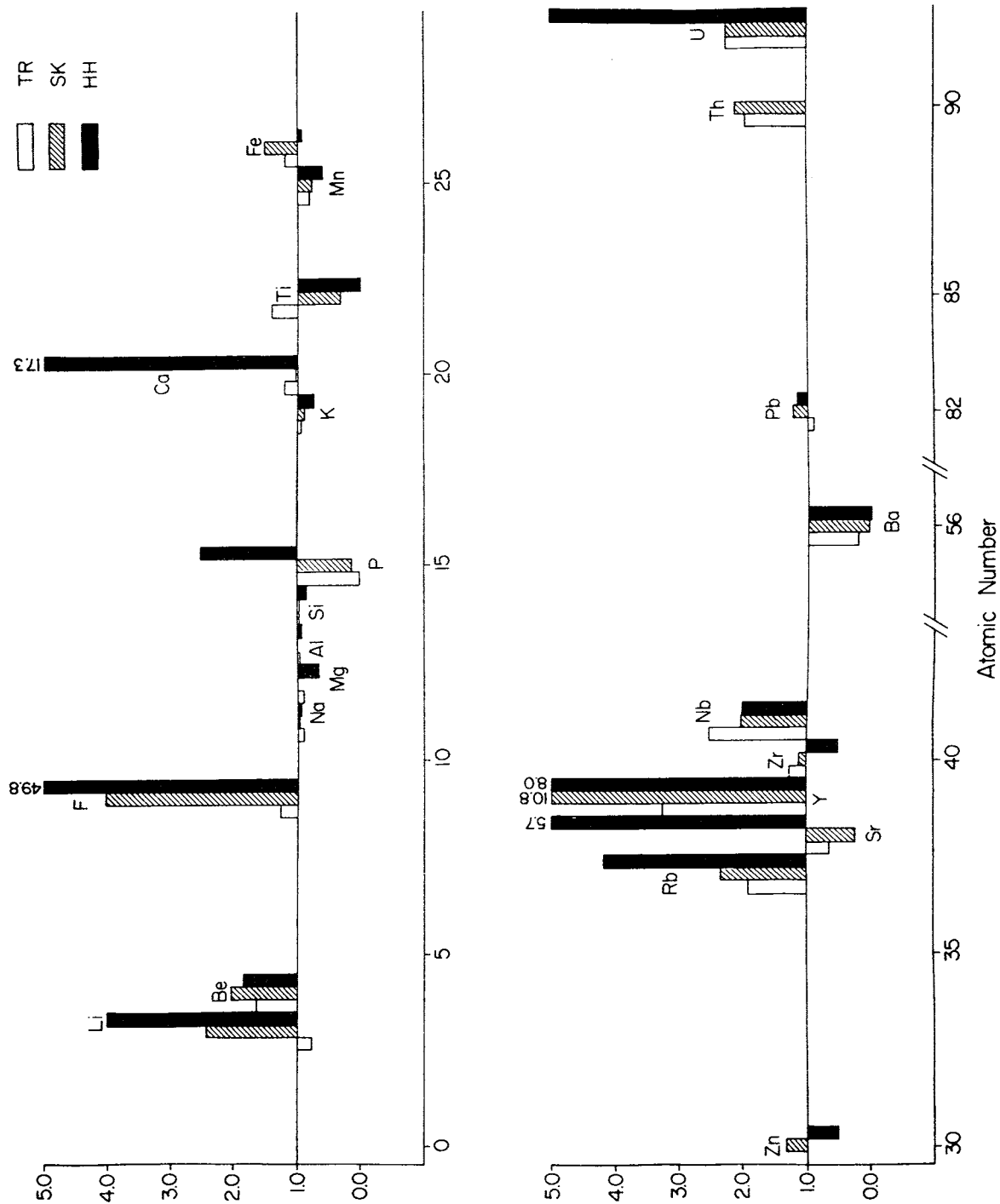


Figure 7. Normalized elemental ratios obtained by dividing whole rock concentrations by those of sample MR74-3 of Evans and Nash (in press). Thomas Range and Smelter Knolls values are averages of all samples; Honeycomb Hills ratios are for HH40 only.

Table 11. X-ray Fluorescence Trace Element Analyses (parts per million)

	HH 40	HH 42	SK 34	SK 45	SK 71	SK 75	TR 21	TR 55	TR 58	TR 79	SK 57	SK 66	SK 72
Li	201	134	102	144	142	102	23	42	14	69	n.d.	n.d.	n.d.
Be	11	13	12	11	14	12	11	10	7	11	n.d.	n.d.	n.d.
Zn	20	25	55	35	65	55	45	40	45	30	45	50	50
Rb	810	1050	455	405	505	460	385	350	335	405	5	5	60
Sr	200	15	5	20	5	5	10	45	30	5	260	310	585
Y	120	105	165	125	185	175	50	60	30	55	25	35	35
Zr	50	90	110	120	110	110	130	125	150	100	90	125	260
Nb	50	80	55	50	55	45	60	60	50	85	5	5	25
Ba	-	-	-	15	-	5	5	110	50	-	670	520	1530
Pb	40	30	45	45	50	30	30	30	30	35	-	-	5
Th	25	50	55	50	55	50	55	55	35	50	-	-	-
U	150	20	10	10	15	10	10	10	15	10	n.d.	n.d.	n.d.
Cl	75	80	960	265	970	940	795	520	580	-	n.d.	n.d.	n.d.

- : not detected

n.d.: not determined

Table 12. Neutron activation analyses of rhyolites (values in ppm except for Fe).

	HH40	HH42	SK34	SK45	SK71	SK75
Sc	3.69±.04	3.87±.04	2.28±0.02	2.19±.02	2.45±.02	2.36±.02
Th	26.83±.27	30.43±.30	58.3±.6	53.1±.5	57.6±.6	56.2±.6
U	151±5	16.66±.17	14.34±.14	9.23±.09	15.27±.15	15.52±.16
Cs	24.37±.24	19.58±.27	20.62±.27	9.95±.15	23.51±.31	19.84±.21
Hf	5.52±.09	6.13±.09	7.57±.10	7.12±.10	7.78±.10	7.38±.10
Fe (%)	.46±.03	0.62±.02	0.85±.02	0.89±.02	0.84±.02	.86±.02
Rb	602±30	1051±35	467±16	432±15	528±18	328±15
Cr	<3.2	2.6±.8	<3.0	2.6±.7	3.4±.8	<3.3
Sb	0.33±.08	1.37±.11	3.42±.20	1.36±.10	3.93±.23	3.67±.23
Mo	<24	3.4±1.7	3.6±1.1	2.8±1.1	2.0±1.7	5.9±1.7
Mn	341±3	343±7	298±6	260±5	338±7	307±7
La	39.4±1.2	49.7±.9	43.5±.8	41.8±.8	36.8±.8	40.3±.08
Ce	103±5	118.7±1.3	103.5±1.1	97.8±1.1	96.1±1.1	95.9±1.3
Nd	43.4±4.4	53.0±1.9	51.6±1.8	47.9±1.7	48.3±1.8	49.4±2.1
Sm	13.2±.4	13.79±.14	13.63±.14	11.75±.12	14.09±.14	14.07±.14
Eu	.047±.009	.041±.009	.111±.009	.146±.009	.080±.009	.082±.009
Tb	2.69±.13	3.00±.15	3.16±.16	2.65±.14	3.41±.17	3.14±.14
Dy	22.8±.23	23.89±.42	24.06±.36	20.46±.36	26.49±.46	25.4±.25
Yb	26.12±.26	27.75±.23	19.38±.19	16.10±.16	21.99±.22	20.76±.21
Lu	-	3.88±.11	2.60±.07	2.20±.06	2.97±.07	2.84±.08

no explanation for the discrepancy; at the present we favor the XRF values because of the precision we have been able to obtain for Rb in a wide variety of samples. HH42 is distinctive, containing over 1000 ppm Rb. Normalized rare earth element concentrations are illustrated in figure 8. Rhyolites from both Honeycomb Hills and Smelter Knolls exhibit a relative enrichment in heavy rare earth elements when compared to less evolved Quaternary rhyolites from the Mineral Mountains (Nash, unpublished data).

In summary, the chemical data show that the Honeycomb Hills rhyolites are the most evolved, followed by Smelter Knolls and the Thomas Range, respectively. This is a purely chemical comparison; age relations and areal separation preclude these areas from being related to a single magma source.

GEOOTHERMOMETRY

Various geothermometers have been devised in an effort to determine groundmass temperatures and temperatures of equilibration between phenocrysts in magma chambers. The two-feldspar geothermometer of Stormer (1975) can be applied to rhyolites (table 13). Calculations were done at a nominal pressure of 100 bars, using directly coexisting feldspars (alkali feldspar and plagioclase in contact with each other) indicated by tie lines in figure 3, and average phenocryst compositions in samples without adjacent plagioclase and alkali feldspars. Temperatures of equilibration for phenocrysts in Thomas Range samples range from 690 to 790°C, whereas Smelter Knolls rhyolites yielded temperatures in the 630 to 685°C range, and Honeycomb Hills rocks crystallized at an unusually low 605°C. Fe-Ti oxide temperatures (Buddington and Lindsley, 1964) are in reasonable agreement with the two-feldspar temperatures: 725°C (Fe-Ti oxide) vs. 695°C (two-feldspar) for TR55, and 665°C vs. 660°C for SK34. The average two-feldspar temperatures for the three areas (Thomas Range: 720°C; Smelter Knolls: 665°C; Honeycomb Hills: 605°C) decrease as their degree of magmatic evolution increases.

The olivine-clinopyroxene geothermometer of Powell and Powell (1974) was applied to groundmass crystals in tholeiitic basalts. The groundmass of sample SK57 crystallized at 1015°C, and SK66 at 1025°C, compared to a 1000°C Fe-Ti oxide temperature for SK66. The plagioclase geothermometer of Kudo and Weill (1970) gives reasonable temperatures (between 900 and 1200°C) at water pressures between 1 and 5 Kb. The revised plagioclase geothermometer of Mathez

(1973) produces reasonable temperatures at a water pressure of 0.5 Kb, but these are approximately 100°C higher than the Kudo-Weill values.

A groundmass temperature of 1070°C was calculated from coexisting orthopyroxene and clinopyroxene (Wood and Banno, 1973) in basaltic andesite, which seemingly is a high temperature for a rock more siliceous than tholeiitic basalt. The Kudo-Weill method gives temperatures of 800 to 1100°C at 1.5Kb H₂O, whereas the Mathez geothermometer again provides its most reasonable temperatures (1000-1140°C) at lower water pressures.

GEOBAROMETRY

Pressure solutions for rhyolitic magmas are approached by calculating water fugacities which are converted to water pressures by interpolating the data of Burnham et al. (1969). This hydrostatic pressure is assumed to equal lithostatic pressure in a closed system in which water constitutes most of the fluid phase. Assuming an average crustal specific gravity of 2.7, a conversion factor of 1 Kbar pressure = 3.83 km lithospheric depth allows the estimation of minimum depths to magma chambers (table 14). Details of the thermodynamic calculations are provided in the appendix.

Sample SK34 yielded a water fugacity of 37 bars, which corresponds to a water pressure of 40 bars and an equivalent lithostatic depth of 0.2 km. TR55 provided values of $f_{H_2O} = 19$ bars, $P_{H_2O} = 20$ bars, and a depth of 0.1 km. According to these data, phenocrysts in Thomas Range and Smelter Knolls rhyolites formed under near-surface conditions. The masses of the extrusive bodies alone (maximum thicknesses of 0.12 km for SK34 and 0.6 km for TR55) are nearly enough to produce the calculated lithostatic pressures.

This geobarometer was not applicable to the Honeycomb Hills rhyolite, where coexisting Fe-Ti oxides were not found. However, the coexisting mineral assemblage plagioclase-fluorite-topaz-quartz-biotite can be used to estimate water fugacities (see appendix). TR79 solutions ranged from 246 bars (siderophyllite) to 501 bars (phlogopite-annite), which correspond to minimum depths of 1.0 and 2.1 km. The calculated water fugacity for SK45 was 729 bars (3.8 km depth), considerably higher than the 37 bars calculated for SK34 by the Wones and Eugster procedure. Comparison of water fugacities for cogenetic crystalline rhyolites and obsidians may not be valid, however; crystalline rhyolites could undergo considerable postmagmatic fluoride-

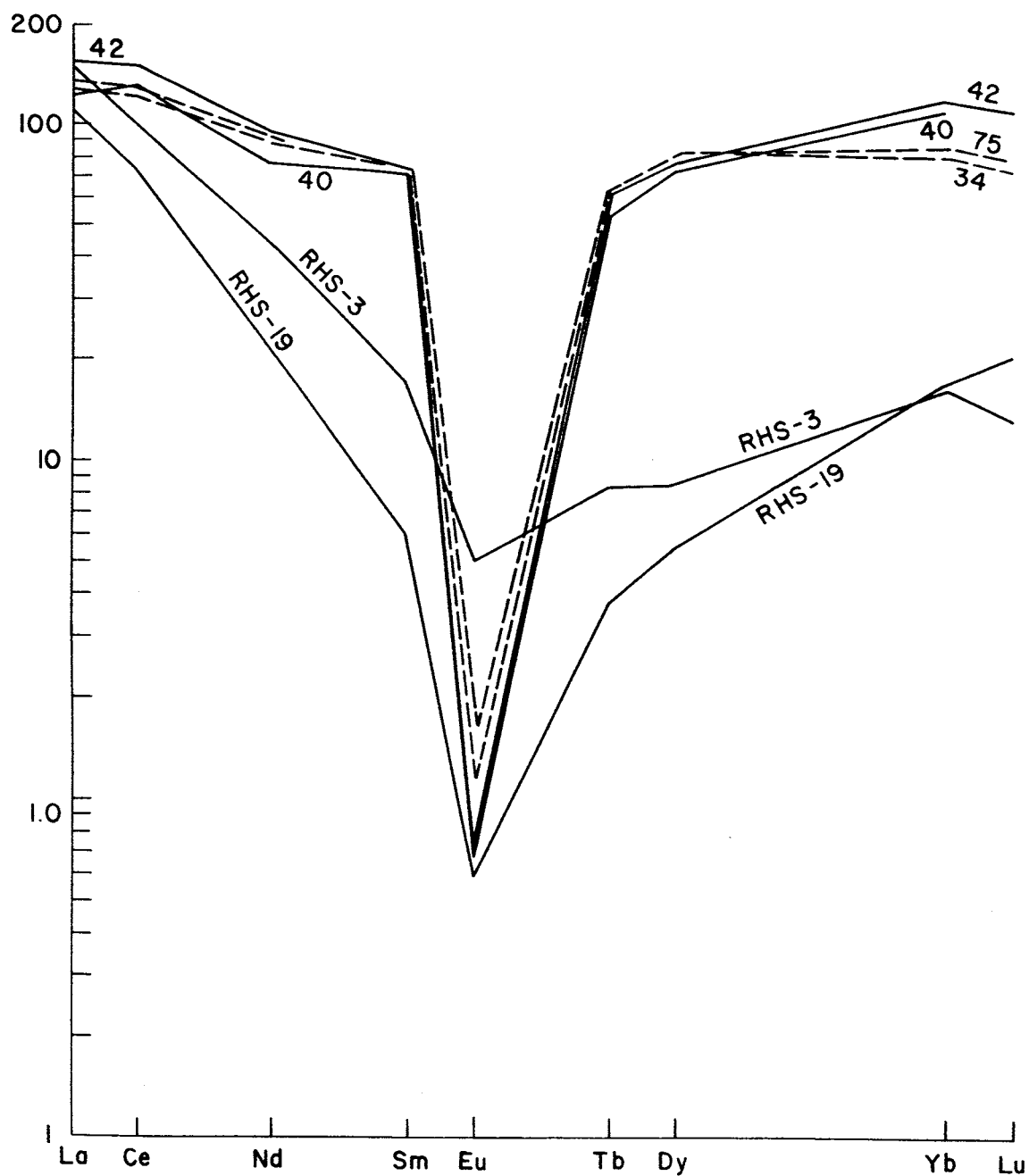


Figure 8. Chondrite-normalized rare earth concentrations for rhyolites from the Honeycomb Hills (solid lines, 40 and 42), Smelter Knolls (dashed lines) and the Mineral Mountains (solid lines RHS-3 and -19).

Table 13. Geothermometry

	HH 40	HH 42	TR 21	TR 55	TR 58	TR 79	SK 34	SK 45	SK 71	SK 75	SK 57	SK 66	SK 72	
Fe-Ti oxides	725			665				1000						
2-Feldspar (100 bars)	605	605	710	695	690	790	660	685	680	630				
Cpx-01												1015	1025	
Cpx-Opx												1070		
Kudo - (1Kb)												1185	1160	1110
Weill (5Kb)												935	905	820
Rev. (0.5Kb)												1110	1080	1005
K.-W. (1Kb)												1225	1200	1140

Table 14. Geobarometry

	HH 40	HH 42	TR 21	TR 55	TR 58	TR* 79	SK 34	SK 45	SK 71	SK 75	SK 66	
$-\log f_{O_2}$	16.6					19.9				10.9		
f_{H_2O} (Wones & Eugster)	19					37						
(bars) (Topaz-Biotite)	166	1001					501	729				
							246					
p_{H_2O} (bars)	185	1870	20			555	40	980				
							255					
Depth (km)	0.7	7.2	0.1			2.1	0.2	3.8				
							1.0					
$-\log \frac{f_{HF}}{f_{H_2O}}$	1.99	2.42	2.72	2.43	3.04	1.71	2.79	2.11	2.59	2.72		
							1.55					
fHF (bars)	1.7	3.8	0.1			9.8	0.1	5.7				
							6.9					

*TR79 values refer to phlogopite-annite (top) and siderophyllite (bottom) - based calculations, respectively.

hydroxyl exchange as compared to rapidly quenched obsidians.

There are several factors complicating water fugacity determinations for rhyolites. The original Wones (1972) free energy function for reaction (1) (appendix) gives values that are roughly three times as high as the values reported here. Water fugacities of 103 bars (SK34) and 64 bars (TR55) derived from the Wones expression can therefore be viewed as upper limits. Munoz and Ludington (1974) acknowledge the probability of significant amounts of oxygen substituting for fluoride or hydroxyl, which will affect the calculated F:OH ratio. Rieder (1971) states that the relationship between F:OH ratio and temperature for biotites may break down at low temperatures and pressures in the presence of significant F, H₂O, and Li. These problems have to be taken into consideration when water fugacity data derived from biotite is to be interpreted.

The Munoz and Ludington (1974) expressions defining OH-F exchange equilibria in biotites can be used to calculate HF:H₂O fugacity ratios. Log $f_{\text{HF}}/f_{\text{H}_2\text{O}}$ ranges from -1.55 to -3.04, with an average of -2.4. Evtiukhina et al. (1967) report a value of -2.56 for a granite melt in equilibrium with HF at a water pressure of 1 Kbar.

HF fugacities were calculated for samples possessing water fugacity data. The fugacity of HF in crystalline rhyolites varied from 1.7 to 9.8 bars. Obsidians gave much lower values (0.1 bar), but this may be a result of the different methods used for calculating water fugacities.

The tholeiitic basalt mineral assemblage lends itself to the estimation of temperatures and pressures of equilibration with mantle materials through the application of the methods of Nicholls and Carmichael (1972), with refinements by Carmichael et al. (1977) and Nicholls (1977). In this procedure, it is assumed that the magma remains at a constant composition from source to the surface. Activities of various components under surface conditions are determined using groundmass mineral compositions. These components are inserted into reactions with postulated mantle minerals, which can then be solved for a set of activity curves in pressure-temperature space. In principle, these curves should intersect at a point representative of the conditions under which the magma equilibrated at its source.

For sample SK66, the Fe-Ti oxide temperature and oxygen fugacity were used along with groundmass

plagioclase, clinopyroxene, and olivine to determine activities of the following components under surface conditions: fayalite (reaction 2, table 15), diopside (reaction 3), albite (reaction 6), silica (reaction 8), and alumina (reaction 7). Utilizing mantle compositions for olivine, orthopyroxene, clinopyroxene, and spinel as given by Carmichael et al. (1977), reactions 1-5 could then be solved to produce a set of activity curves.

This procedure yielded the set of curves shown in figure 9. Curve 3 intersects reasonably with curves 1 and 5 at approximately 20 Kb and 1350-1400°C. Unfortunately, curve 2 (fayalite) is displaced well to the high-temperature side of this intersection. Curve 2 was generated with an average groundmass olivine composition of Fa₃₆; utilization of the most magnesian groundmass olivine (Fa₂₈) shifts the curve only 100°C to the left. On this evidence, it can be concluded that the lava in its present composition was not in equilibrium with normal mantle material, and that the assumptions of equilibrium and unchanged composition from the source area to the surface do not apply to this magma.

GEOHERMAL RESOURCE POTENTIAL

Smith and Shaw (1975) consider shallow silicic magma chambers to be the primary heat sources for geothermal systems. They have devised a method for evaluating the geothermal potential of an igneous complex based on the age of the youngest eruption and the size of the magma chamber beneath the surface (estimated by multiplying the erupted volume of rhyolite by a factor of 10). On this basis, all three rhyolitic systems considered here have little apparent geothermal potential, mostly because of their relatively old ages of eruption.

One warm (49°C) spring occurs near the northern end of the Thomas Range (Staatz and Carr, 1964). This water could merely be heated by the normal geothermal gradient as it circulates along deep faults. No active hot springs or recent hot spring deposits are known in the Honeycomb Hills and Smelter Knolls areas. However, two features of the Smelter Knolls area are of geothermal interest. One feature is its apparent structural continuity with Fumarole Butte, which has active hot springs to its east. The other is young (0.31 m.y.) basaltic volcanism nearby which could have provided an influx of heat into a previously dormant rhyolitic system. Heat flow measurements at Smelter Knolls would be of value in a continued exploration program.

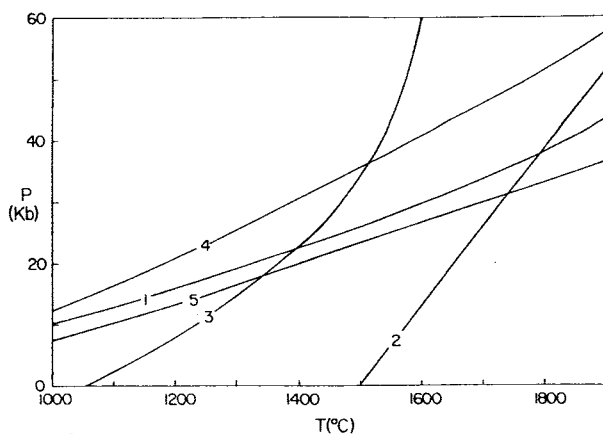


Figure 9. Equilibration curves between lava SK66 and the postulated mantle composition of Carmichael et al. (1977). Numbered curves refer to reactions given in table 15.

Table 15. Reactions used to define the activities of components in silicate melts

No.	Reaction	Component
1	$Mg_2SiO_4 + SiO_2 = Mg_2Si_2O_6$ Olivine Melt Orthopyroxene	SiO_2
2	$Fe_2SiO_4 = Fe_2SiO_4$ Melt Olivine	Fe_2SiO_4
3	$CaMgSi_2O_6 = CaMgSi_2O_6$ Melt Clinopyroxene	$CaMgSi_2O_6$
4	$Mg_2SiO_4 + Al_2O_3 = 1/2Mg_2Si_2O_6 + MgAl_2O_4$ Olivine Melt Orthopyroxene Spinel	Al_2O_3
5	$NaAlSi_3O_8 + Mg_2SiO_4 = Mg_2Si_2O_6 + NaAlSi_2O_6$ Melt Olivine Orthopyroxene Clino- pyroxene	$NaAlSi_3O_8$
6	$NaAlSi_3O_8 = NaAlSi_3O_8$ Melt Feldspar	$NaAlSi_3O_8$
7	$CaMgSi_2O_6 + Al_2O_3 + 1/2SiO_2 = CaAl_2Si_2O_8 + 1/2Mg_2SiO_4$ Clinopyroxene Melt Melt Feldspar Olivine	Al_2O_3, SiO_2
8	$2/3Fe_3O_4 + SiO_2 = Fe_2SiO_4 + 1/3O_2$ Magnetite Melt Olivine Gas	SiO_2

PETROGENESIS

The genetic model for these rhyolites is similar to that proposed by Evans (1978) for the rhyolites of the Mineral Range, 90 km to the south. High regional heat flow (Sass, 1976) and periodic injections of basaltic magma into the crust have resulted in melting of granitic crustal material and subsequent eruption of rhyolite. Heat flow and the ascent of basalt from the upper mantle is facilitated by the thin crust (25-30 km) in the area. The high degree of chemical differentiation of these rhyolites indicates considerable residence time within magma chambers.

Lindsey (1977) speculates that the Honeycomb Hills represent the top of a buried plutonic system. The extremely evolved composition indicates that the lavas are products of a residual (pegmatitic) magma with a larger body of less evolved magma at depth. High fluorine contents at this locality may be evidence of a plutonic roof zone (Bailey, 1977).

The Smelter Knolls also exhibit the characteristics of a body of pegmatitic magma derived from a shallow source. Recent faulting and basaltic volcanism suggest that this area may still be tectonically active. The Thomas Range rhyolites have emptied a much larger subsurface volume than the other areas, which could have resulted in the formation of a postulated collapsed caldera structure (Shawe, 1972).

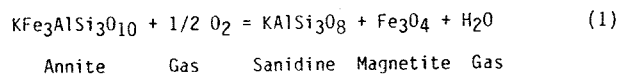
ACKNOWLEDGMENT

Funding for this research was provided by U. S. Geological Survey grant 14-08-0001-G-343. F. H. Brown, S. H. Evans, Jr., and J. B. Petersen provided valuable assistance and advice regarding age dating and chemical analyses. Neutron activation analyses were performed by F. Asaro, Lawrence Berkeley Laboratories; funding for these analyses was provided by Department of Energy, Division of Geothermal Energy, contract EG-78-C-07-1701.

APPENDIX

A. H₂O FUGACITY CALCULATIONS.

The mineral-vapor phase reaction:



Wones and Eugster, 1965 allow for the calcula-

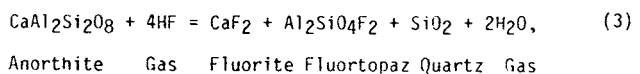
tion of water fugacities in the rhyolite magmas as follows:

$$\log f_{H_2O} = \frac{8673}{T} + 2.46 + 1/2 \log f_{O_2} + \log \chi_{Fe^{2+}}^{biotite} \quad (2)$$

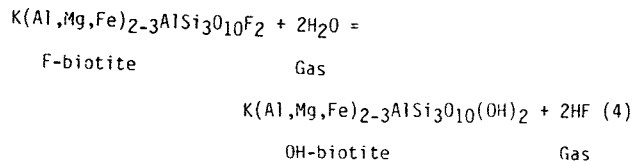
$$+ 2 \log \chi_{OH}^{biotite} - \log a_{san} - \log a_{mt}$$

Sanidine activities were taken from Carmichael et al. figure 4-30), (1974, whereas magnetite activity is assumed to be equivalent to mole fraction. Annite activity is the cube of the mole fraction (Wones, 1972) and the OH term takes into account an assumed ideal mixing of fluorine in the hydroxyl site. Temperatures and oxygen fugacities were provided by coexisting Fe-Ti oxides (table 13). The free energy function is that advocated by Hildreth (1977) and is based upon a reevaluation of the original experimental data of Wones and Eugster (1965). If reaction (1) acts as a control on biotite composition, low oxygen fugacities (SK34 log f_{O_2} = -19.9) are probably responsible for the iron-rich biotites at Smelter Knolls and Honeycomb Hills.

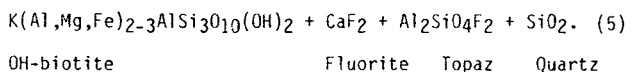
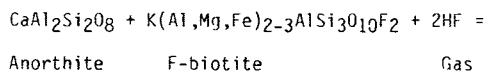
The assemblage plagioclase-fluorite-topaz-quartz-biotite may be used to estimate water fugacities. The reaction:



when combined with the biotite exchange reaction



Yields:



The equilibrium constant for the above reaction is given by

$$K^{(5)} = \frac{(OH-biotite) (Fluorite) (Fluortopaz) (Quartz)}{(Anorthite) (F-biotite) (HF)^2}$$

Where quantities in parentheses denote activities. Using the relation $\Delta G_r^\circ = -RT \ln K$, and assuming unit activities for fluorite, fluortopaz, and quartz,

$$\ln K_{(5)} = \frac{\Delta G^\circ(5)}{-RT} = \ln \left[\frac{(\text{OH-bio})}{(\text{F-bio})} \right] - \ln \left[(\text{An})(\text{HF})^2 \right],$$

and

$$\ln(\text{HF}) = 1/2 \ln \left[\frac{(\text{OH-bio})}{(\text{F-bio})} \right] - \frac{\ln(\text{An})}{2} + \frac{\Delta G^\circ(5)}{2RT} \quad (6)$$

For reaction (4),

$$K_{(4)} = \frac{(\text{OH-bio})(\text{HF})^2}{(\text{F-bio})(\text{H}_2\text{O})^2}$$

therefore,

$$\ln K_{(4)} = \frac{\Delta G^\circ(4)}{-RT} = \ln \left[\frac{(\text{OH-bio})}{(\text{F-bio})} \right] + 2 \ln(\text{HF}) - 2 \ln(\text{H}_2\text{O}),$$

and

$$\ln(\text{H}_2\text{O}) = 1/2 \ln \left[\frac{(\text{OH-bio})}{(\text{F-bio})} \right] + \frac{\Delta G^\circ(4)}{2RT} + \ln(\text{HF})$$

Substituting equation (6) for HF fugacity gives

$$\ln(\text{H}_2\text{O}) = \ln \left[\frac{(\text{OH-bio})}{(\text{F-bio})} \right] - \frac{\ln(\text{An})}{2} + \frac{\Delta G^\circ(4) + \Delta G^\circ(5)}{2RT} \quad (7)$$

The cation activity ratio in the biotite term will equal unity since only OH-F exchange is being considered. This term can be simplified further by assuming that OH and F mix ideally on two sites. Therefore,

$$\ln \left[\frac{(\text{OH-bio})}{(\text{F-bio})} \right] = \ln \left[\frac{(x_{\text{OH}}^{\text{bio}})^2}{(x_{\text{F}}^{\text{bio}})^2} \right],$$

and

$$\ln(\text{H}_2\text{O}) = 2 \ln \left[\frac{x_{\text{OH}}^{\text{bio}}}{x_{\text{F}}^{\text{bio}}} \right] - \frac{\ln(\text{An})}{2} + \frac{\Delta G^\circ(4) + \Delta G^\circ(5)}{2RT} \quad (8)$$

Since

$$\Delta G^\circ(5) = \Delta G^\circ(4) + \Delta G^\circ(3)$$

the final expression can be written as:

$$\ln(\text{H}_2\text{O}) = 2 \ln \left[\frac{x_{\text{OH}}^{\text{bio}}}{x_{\text{F}}^{\text{bio}}} \right] - \frac{\ln(\text{An})}{2} + \frac{(2\Delta G^\circ(4) + \Delta G^\circ(3))}{2RT} \quad (9)$$

Anorthite activity is considered to equal mole fraction anorthite in plagioclase. The free energy change for reaction (3) was evaluated using data for anorthite, fluorite, and quartz from Robie and Waldbaum (1968).

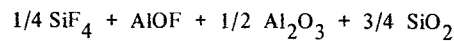
HF and H₂O free energies were taken from Stull and Prophet (1971). Free energy data for fluortopaz was estimated using the method of Chen (1975) which is described below. For reaction (3) the equilibrium constant varies with temperature as follows:

$$\ln K^\circ(3) = \frac{-\Delta G^\circ(3)}{RT} = \frac{29710}{T} - 22.996$$

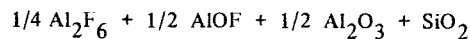
The approximate mineral assemblage for the application of this method is present in HH40, HH42, and SK45. The relationship was also applied to TR79, although topaz occurs only as a lithophysal mineral in this sample. Munoz and Ludington (1974) offer equations for evaluating the free energy change of reaction (4) whether the biotite in question is a phlogopite, annite, siderophyllite, or an intermediate phlogopite-annite. Because Honeycomb Hills biotites contain considerable octahedral Al and very little Mg, they were treated as siderophyllites. SK45 biotite was calculated as a mixed phlogopite-annite. TR79 biotite, with significant amounts of both octahedral Al and Mg, was evaluated both as a siderophyllite and as a mixed phlogopite-annite.

B. ESTIMATION OF THE FREE ENERGY OF FORMATION OF FLUORTOPAZ

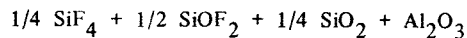
The free energy of formation of fluortopaz was estimated with the method of Chen (1975). The components SiF₄, AlOF, Al₂O₃, SiO₂, SiOF₂, Al₂F₆, and AlF₃ were combined in the following ways to form the fluortopaz molecule (Al₂SiO₄F₂):



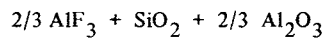
$$\Sigma G_{f,298}^\circ = -576.875 \frac{\text{Kcal}}{\text{mol}}$$



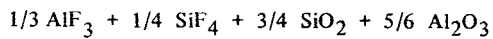
$$\Sigma G_{f,298}^\circ = -616.330 \frac{\text{Kcal}}{\text{mol}}$$



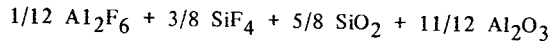
$$\Sigma G_{f,298}^\circ = -636.835 \frac{\text{Kcal}}{\text{mol}}$$



$$\Sigma G_{f,298}^\circ = -646.805 \frac{\text{Kcal}}{\text{mol}}$$



$$\Sigma G_{f,298}^\circ = -657.580 \frac{\text{Kcal}}{\text{mol}}$$



$$\sum_{f,298} G^\circ = -666.260 \frac{\text{Kcal}}{\text{mol}}$$

Free energy summations for these combinations were obtained from data given in Robie and Waldbaum (1968) and Stull and Prophet (1971). These free energy sums were arranged in descending order as ordinate values, and each was assigned an integer abscissa value ranging from 0 for the greatest (least negative) value to 5 for the lowest (most negative) value. These points were then fit by a nonlinear least-squares process to an equation of the form

$$Y = ae^{bx} + c$$

where c , the asymptotic limit of the equation, represents an extrapolated free energy value which should approach the true value for the substance being studied. This value was determined at temperatures from 298 to 1500°K. A linear least-squares fit to these data produced the following fluorotopaz free-energy function:

$$\frac{\Delta G^\circ_f}{RT} = \frac{-355.77}{T} + 57.83.$$

REFERENCES

- Armstrong, R. L., 1970, Geochronology of Tertiary igneous rocks, eastern Basin and Range Province, western Utah, eastern Nevada, and vicinity, U.S.A: *Geochim. Cosmochim. Acta* 34, p. 202-232.
- Bailey, J. C., 1977, Fluorine in granitic rocks and melts: a review: *Chem. Geol.* 19, p. 1-42.
- Best, M. G., W. H. Brimhall, 1974, Late Cenozoic alkalic basaltic magmas in the western Colorado Plateau and the Basin and Range transition zone, U. S. A., and their bearing on mantle dynamics: *Geological Society American Bulletin* 85, p. 1677-1690.
- Buddington, A. F., D. H. Lindsley, 1964, Iron-titanium oxide minerals and synthetic equivalents. *J. Petrol.* 5, p. 310-357.
- Burnham, C. W., J. R. Holloway, N. F. Davis, 1969, Thermodynamic properties of water to 1,000°C and 10,000 Bars: *Geological Society of America Special Paper* 132, 96 p.
- Carmichael, I. S. E., J. Hample and R. N. Jack, 1968, Analytical data on the U. S. G. S. standard rocks: *Chemical Geology* 3, 59-64.
- Carmichael, I. S. E., F. J. Turner, J. Verhoogen, 1974, *Igneous Petrology*: McGraw-Hill, New York, 739 p.
- Carmichael, I. S. E., J. Nicholls, F. J. Spera, B. J. Wood, S. A. Nelson, 1977, High temperature properties of silicate liquids: Applications to the equilibration and ascent of basic magma: *Trans. Royal Society London, Series A286*, p. 373-431.
- Caskey, C. F., 1975, The Needles Range Formation in southwest Utah: paleomagnetism and stratigraphic correlation: Ph.D. Thesis, University of Utah, 106 p.
- Chen, C., 1975, A method of estimation of standard free energies of formation of silicate minerals at 298.15°K: *American Journal Science* 275, p. 801-817.
- Christiansen, R. L., P. W. Lipman, 1966, Emplacement and thermal history of a rhyolite lava flow near Fortymile Canyon, southern Nevada: *Geologic Society America Bulletin* 77, p. 671-684.
- Erickson, M. P., 1963, Volcanic geology of western Juab County Utah: *Utah Geological Society Guidebook to the Geology of Utah*, no. 17, Beryllium and uranium mineralization in western Juab County, Utah, ed. B. J. Sharp and N.C. Williams, p. 23-35.
- Evans, S. H., Jr., 1978, Studies in Basin and Range volcanism. Unpub. Ph.D. thesis, University of Utah, 119 p.
- Evtiukhina, I. A., L. N. Kogarko, L. L. Kunin, V. I. Malkin, L. N. Rudchenko, 1967, Acid-base properties of some aluminosilicate melts, simplified analogues of natural rocks: *Dokl. Akad. Nauk, S.S.S.R.*, 175, p. 1369-1371.
- Fisher, R. A., 1953, Dispersion on a sphere: *Proc. Royal Society London, Series A217*, p. 295-305.
- Foster, M. D., 1964, Water content of micas and chlorites: U. S. Geological Survey Professional Paper 474-5, 15 p.
- Glyuk, D. S., V. N. Anfilogov, 1973, Phase equilibria in the system granite-H₂O-HF at a pressure of 1000Kg/cm²: *Geokhimiya* 3, p. 434-438.
- Green, T. H., A. E. Ringwood, 1968, Genesis of the calc-alkaline igneous rock suite: *Contrib. Mineral. Petrol.*, 18, p. 105-162.
- Haggerty, S. E., 1976, Oxide Minerals: *Mineralogical Society of America Short Course Notes*, v. 3, p. Hg-101-Hg-300.
- Hausel, W. D., W. P. Nash, 1977, Petrology of Tertiary and Quaternary volcanic rocks, Washington County, southwestern Utah: *Geological Society America Bulletin* 88, 1831-1842.
- Heming, R. F., 1977, Mineralogy and proposed P-T paths of basaltic lavas from Rabaul Caldera, Papua, New Guinea: *Contrib. Mineral. Petrol.*, 61, p. 15-33.
- Hildreth, E. W., 1977, The Magma chamber of the Bishop Tuff; Gradients in temperature, pressure, and composition: Ph.D. Thesis, University of California, Berkeley, 328 p.
- Hintze, L. F., 1973, Geologic History of Utah: *Brigham Young University Geology Studies*, v. 20, Pt. 3, 181 p.

- Hogg, N. C., 1972, Shoshonitic lavas in west central Utah: Brigham Young University Geology Studies, 19, Pt. 2, p. 133-184.
- Kogarko, L. N., L. D. Krigman, 1973, Structural position of fluorine in silicate melts, based on melting diagram data: *Geokhimiya*, 1, p. 49-56.
- Kovalenko, V. I., M. I. Kuzmin, V. S. Antipin, L. L. Petrov, 1971, Topaz-bearing quartz keratophyre (ongonite), a new variety of subvolcanic igneous dike rocks: *Doklady Akad. Nauk, S.S.S.R.*, t. 199, No. 2, p. 430-433.
- Kudo, A. M., and D. F. Weill, 1970, An igneous plagioclase thermometer: *Contrib. Mineral. Petrol.*, 25, p. 52-65.
- Lindsey, D. A., 1977, Epithermal beryllium deposits in water-laid tuff, western Utah: *Econ. Geol.*, 72, p. 219-232.
- Lipman, P. W., R. L. Christiansen, R. E. Van Alstine, 1969, Retention of alkalis by calc-alkalic rhyolites during crystallization and hydration: *Amer. Mineral.*, 54, p. 286-291.
- Mathez, E. A., 1973, Refinement of the Kudo-Weill plagioclase thermometer and its application to basaltic rocks: *Contrib. Mineral. Petrol.*, 41, p. 61-72.
- McAnulty, W. N., A. A. Levinson, 1964, Rare alkali and beryllium mineralization in volcanic tuffs, Honeycomb Hills, Juab County, Utah: *Econ. Geol.* 59, p. 768-774.
- McDougall, I., 1977, The present status of the geomagnetic polarity time scale: *Australian Nat. University Research School of Earth Sciences, Pub. no. 1288*, 34 p.
- Munoz, J. L., S. D. Ludington, 1974, Fluoride-hydroxyl exchange in biotite: *American Journal Science*, 274, p. 396-413.
- Nicholls, J., 1977, The activities of components in natural silicate melts: in Frazer, D. G., ed., *Thermodynamics in Geology*, D. Reidel Pub. Co., Holland, p. 327-349.
- Noble, D. C., V. C. Smith, L. C. Peck, 1967, Loss of halogens from crystallized and glassy silicic volcanic rocks: *Geochim. Cosmochim. Acta* 31, p. 215-223.
- Penfield, S. L., J. C. Minor, Jr., 1894, Veber die chemische Zusammensetzung des Topas und deren Beziehung zu seinen physikalischen Eigenschaften: *Zeit. Krist.* 23, p. 321-329.
- Peterson, J. B., and W. P. Nash, 1980, *Geology and petrology of the Fumarole Butte volcanic complex: This volume.*
- Powell, M., R. Powell, 1974, An olivine-clinopyroxene geothermometer: *Contrib. Mineral. Petrol.* 48, p. 249-263.
- Rieder, M., 1971, Stability and physical properties of lithium-iron micas: *Amer. Mineral.*, 56, p. 256-280.
- Robie, R. A., D. R. Waldbaum, 1968, *Thermodynamic properties of minerals and related substances at 298.15° (25.0°C) and one atmosphere (1.013 bars) pressure and at higher temperatures: U. S. Geol. Survey Bulletin 1259*, 256 p.
- Rosholt, J. N., Prijana, D. C. Noble, 1971, Mobility of uranium and thorium in glassy and crystallized silicic volcanic rocks: *Econ. Geol.* 66, p. 1061-1069.
- Sass, J. H., W. H. Diment, A. H. Lachenbruch, B. V. Marshall, R. J. Munroe, T. H. Moses, Jr., T. C. Urban, 1976, A new heat flow contour map of the conterminous United States: *U. S. Geol. Survey Open File Report 76-756*, p. 24.
- Shapiro, L., 1975, *Rapid analysis of silicate, carbonate, and phosphate rocks - revised ed.: U. S. Geol. Survey Bull.* 1401, 76 p.
- Shawe, D. R., 1966, Arizona-New Mexico and Nevada - Utah beryllium belts: *U.S. Geol. Survey Prof. Paper 550-C*, p. C206-213.
- _____, 1972, Reconnaissance geology and mineral potential of Thomas, Keg, and Desert Calderas, central Juab County, Utah: *U. S. Geol. Survey Prof. Paper 800-B*, p. B67-B77.
- Shell, H. R., R. L. Craig, 1954, Determination of silica and fluoride in fluorosilicates: *Anal. Chem.*, 26, p. 996-1001.
- Smith, R. L., H. R. Shaw, 1975, *Igneous-related geothermal systems in Assessment of Geothermal Resources of the United States - 1975: U.S. Geol. Survey Circular 726*, D. F. White and D. L. Williams, Ed., 155 p.
- Staatz, M. H., W. J. Carr, 1964, *Geology and mineral deposits of the Thomas and Dugway Ranges, Juab and Tooele Counties, Utah: U. S. Geol. Survey Prof. Paper 415*, 188 p.
- Stormer, J. C., Jr., 1975, A practical two-feldspar geothermometer: *American Mineral.*, 60, p. 667-674.
- Stull, D. R., H. Prophet, et al., 1971, *JANAF Thermochemical Tables: NSRDS-Nat. Bureau Stds.*
- Tuttle, O. F., N. L. Bowen, 1958, Origin of granite in the light of experimental studies in the system NaAlSi₃O₈-KAISi₃O₈-SiO₂-H₂O: *Geol. Soc. Amer. Memoir* 74, 153 p.
- Von Platen, H., 1965, Kristallisation granitischer Schmelzen: *Beitr. Mineral. Petrogr.*, 11, p. 334-381.
- Von Platen, H., H. G. F. Winkler, 1961, Kristallisation eines Obsidians bei Anwesenheit von H₂O, NH₃, HCl, and HF unter 2000 Atm: *Druck. Fortschr. Mineral.*, 39, p. 355.
- Wender, L. E., W. P. Nash, 1979, *Petrology of Oligocene and early Miocene calc-alkalic volcanism in the Marysvale area, Utah: Geol. Soc. Amer. Bull. Part II, v. 90*, p. 34-76.
- Wones, D. R., 1972, Stability of biotite: a reply: *Amer. Mineral.* 57, p. 316-317.
- Wones, D. R., H. P. Eugster, 1965, Stability of biotite-experiment, theory, and application: *Am. Mineral.* 50, p. 1228-1272.
- Wood, B. J., S. Banno, 1973, Garnet-orthopyroxene and ortho-

- pyroxene-clinopyroxene relationships in simple and complex systems: *Contrib. Mineral. Petrol.*, 42, p. 409-424.
- Wyllie, P. J., D. F. Tuttle, 1961, Experimental investigation of silicate systems containing two volatile components, II. The effects of NH_3 and HF , in addition to H_2O , on the melting temperatures of albite and granite: *Am. J. Sci.*, 259, p. 128-143.
- Yakubovick, K. I., A. M. Portnov, 1967, Strontium as a geochemical indicator of genetic connection between mineralization and alkalic rocks: *Dok. Acad. Sci., U.S.S.R., Earth Sci. Sect.*, 175, p. 185-186.
- Zielinski, R. A., P. W. Lipman, H. T. Millard, 1977, Minor-element abundances in obsidian, perlite, and felsite of calc-alkalic rhyolites: *Amer. Mineral.*, 62, p. 426-437.

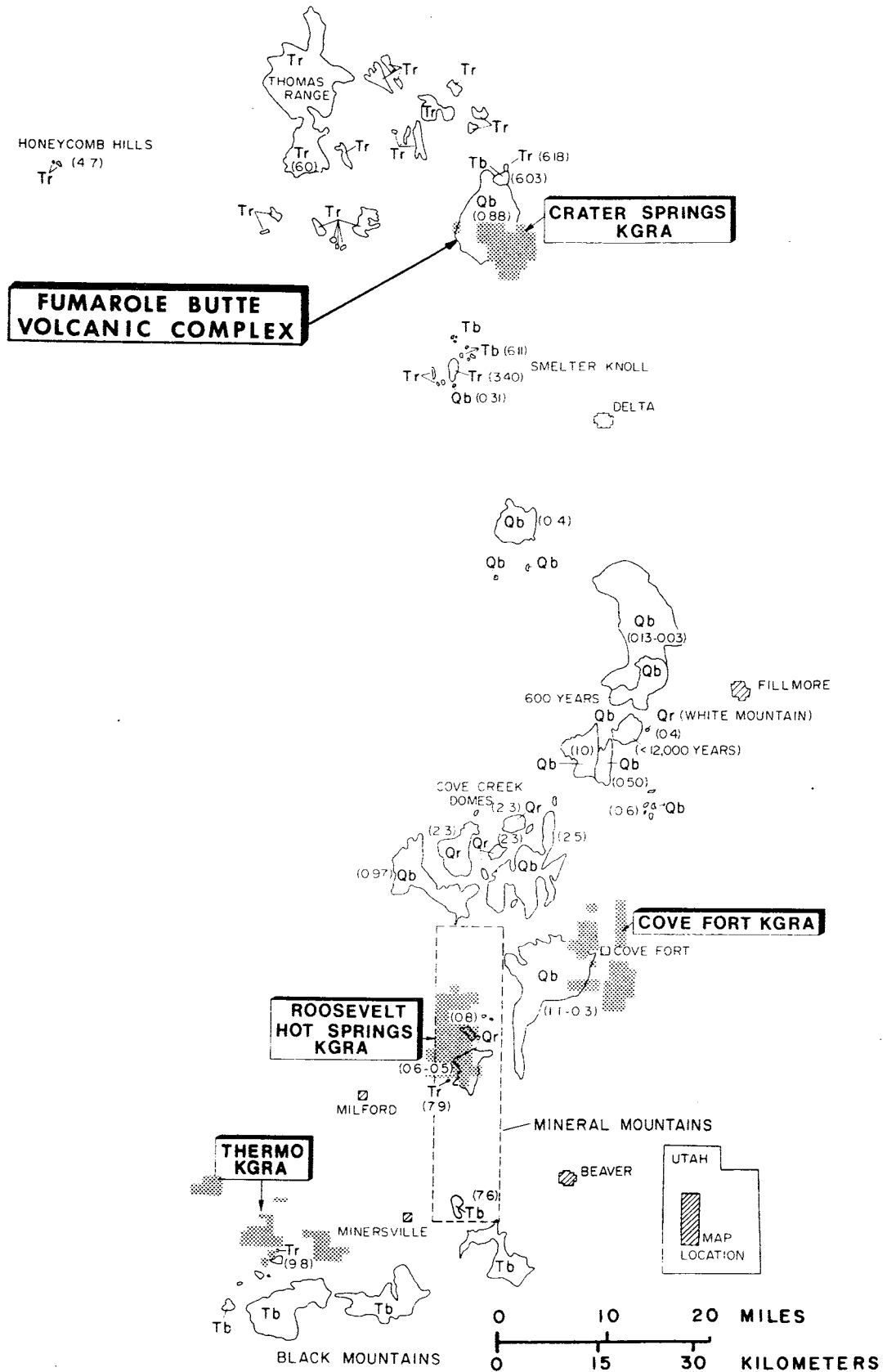


Figure 1. Distribution of late Tertiary and Quaternary volcanic rocks in west-central Utah. Ages are shown in millions of years. Qb = Quaternary basalt, Qr = Quaternary rhyolite, Tb = Tertiary basalt, Tr = Tertiary rhyolite. Known Geothermal Resource Area (KGRA) administrative units are shown as shaded areas.

STUDIES IN LATE CENOZOIC VOLCANISM IN WEST-CENTRAL UTAH

II. GEOLOGY AND PETROLOGY OF THE FUMAROLE BUTTE VOLCANIC COMPLEX, UTAH

by James B. Peterson¹ and W. P. Nash²

ABSTRACT

The Fumarole Butte volcanic complex is located in west-central Utah. Constituting part of a Known Geothermal Resource Area, the complex covers about 105 km² and consists of a shield volcano composed of basaltic andesite, a body of tholeiitic basalt, and a rhyolite flow with two small exposures of obsidian. The basaltic andesite, tholeiite, and rhyolite have been dated at 0.88, 6.0, and 6.1 m.y., respectively, using standard K-Ar age-dating techniques.

The mineralogy of the basaltic andesite and tholeiite indicates that they underwent fractional crystallization at relatively shallow depth. This is supported by the low Al and Na contents of pyroxenes in both rock types, and by thermodynamic calculations applied to the tholeiite. The rhyolite may have been erupted from a shallow depth; calculations for water fugacity indicate minimum depths of about 1 km for the formation of phenocryst minerals.

Crater Springs, located adjacent to the volcano, produce surface water temperatures of 87°C to 90°C, and the waters yield a Na-K-Ca temperature of 155°C. The heat source may be related to igneous activity, but is more likely due to deep circulation along faults in this area of high regional heat flow. High-angle, normal faults are present at Fumarole Butte and have affected the locus of volcanism throughout this area over the past 6 m.y. The fault system appears to extend at least 10 km south to the Smelter Knolls volcanic area, and may be linked to extensive faulting and associated Cenozoic volcanism that occurs throughout areas to the south.

INTRODUCTION

The Fumarole Butte volcanic complex is located in west-central Utah about 40 km northwest of the town of Delta (see figure 1). The volcanic complex consists of a

shield volcano and older, adjacent flows of tholeiitic basalt and rhyolite. Crater Springs (also known as Baker and Abraham hot springs), which lie adjacent to the volcano, are a designated Known Geothermal Resource Area. The thermal spring activity, relatively young appearance of the volcano, presence of siliceous volcanism, and surface expression of a significant fault system make the area a reasonable target for geothermal exploration. A petrologic and petrographic study of the Fumarole Butte volcanic complex was designed to evaluate the geothermal potential of this area through investigation of the age, extent, mineralogy, and chemistry of the associated volcanic rocks.

A number of geological and geophysical studies have been conducted at Fumarole Butte and throughout the surrounding areas. Gilbert (1890) discussed Fumarole Butte in his classic investigation of Lake Bonneville. The Fumarole Butte basalts were mentioned briefly by Erickson (1963) and Shaw (1972) in regional evaluations which included this area. Hogg (1972) conducted a study of the petrology and chemistry of mid-Tertiary and Quaternary volcanics in west-central Utah in which he included the Fumarole Butte volcanics. Smith (1974) completed a gravity survey of Fumarole Butte and adjacent areas, and Johnson (1975) conducted a resistivity and induced polarization survey over Fumarole Butte.

GEOLOGY

Regional Geology

The Fumarole Butte volcanic complex is located within the Basin and Range physiographic province, which is characterized by extensive normal faulting, widespread Tertiary and Quaternary volcanism, abundant thermal spring activity, and high heat flow. Seismic studies indicate that this area has an abnormally thin crust and anomalously low seismic velocities in the underlying mantle (Pakiser, 1965). Such features appear to be consistent with postulated unusually high temperatures at the crust-mantle boundary (Roy *et al.*, 1968).

¹Federal Resources Corp., Salt Lake City, Utah

²Department of Geology and Geophysics, University of Utah, Salt Lake City, Utah 84112.

Local Geology

The Fumarole Butte volcanic complex consists of a shield volcano composed of basaltic andesite, a body of tholeiitic basalt, and a small rhyolite flow with two very small outcrops of obsidian representing a carapace. A geologic map is presented in figure 2.

The shield volcano covers about 100 square kilometers. A volcanic neck, from which the name "Fumarole Butte" was derived, is located in the central-western portion of the volcano and rises about 30 meters above the gentle slope of the shield. The present extent of the volcanic neck probably outlines only the core of the original feature. The area around the neck is marked with red scoria and agglutinate. Portions of the volcano are covered with thin outliers of sediments.

A flow of tholeiitic basalt is located directly north of Fumarole Butte. The tholeiite, referred to as "North Butte" by Hogg (1972), rises topographically above and may be easily distinguished from Fumarole Butte. The tholeiite is about 5 to 8 meters thick and covers about 5 square kilometers. Fumarole Butte lavas have flowed around the margin of North Butte.

A small rhyolite flow is located directly north of and stratigraphically below the tholeiite. Two small outcrops of obsidian occur above the crystalline rhyolite flow and probably represent its outer carapace.

A conglomerate underlies the tholeiite and is exposed along the northeastern margin of Fumarole Butte between the two flows. The conglomerate is reddish-brown in color and contains material that ranges in size from sand grains to large boulders. The conglomerate is composed mainly of white to pink quartzite with a smaller amount of gray limestone and minor amounts of pumice, rhyolite, and basalt that are cemented by calcium carbonate. Generally, the conglomerate strikes about N 20° W and dips about 12° to the east. A second conglomerate is located stratigraphically higher on North Butte.

Beach deposits left by Lake Bonneville are present on North Butte, one of which has obscured the contact between the rhyolite flow and the tholeiite at the 4800' (Provo) level. Minor lacustrine deposits are also present on Fumarole Butte, but beach development is not apparent there. Broad, relatively flat areas that generally lie near the 4800' level are present across Fumarole Butte. Algal limestone which in places contains gastropod shells is present on both Fumarole Butte and North

Butte, indicating that Lake Bonneville once covered a major portion of the Fumarole Butte volcanic complex.

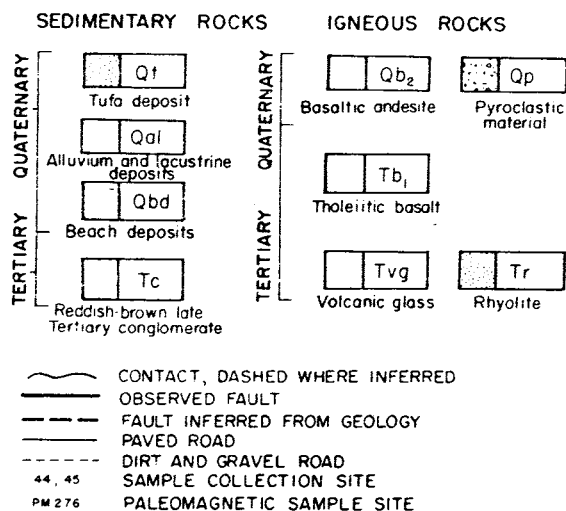
Smith (1974) conducted a gravity survey over and adjacent to the Fumarole Butte volcanic complex. His work reveals a northeast-southwest trending gravity gradient across the west half of Fumarole Butte and an elongate gravity high over Crater Springs. The gravity high over Crater Springs is interpreted by Smith (1974) as an intrusive dike. Smith's model proposes that a basement flexure exists at depth beneath the volcanic complex and that about 2,500 meters of vertical offset occurs at the proposed flexure. The top of the flexure shows good horizontal correlation with the location of the volcanic neck and may indicate a fracture system at depth through which basaltic material was extruded from a deep crustal environment to the surface.

Johnson (1975) conducted an induced polarization and resistivity survey at Fumarole Butte. He attempted to delineate the contact between the basalt and the underlying sediments, determine the thickness of the basalt, and outline the magma source. He determined that the thickness of the basaltic andesite ranged from 75 to 90 meters in an area about 1,000 meters southwest of the volcanic neck, and approximately 45 meters in an

GEOLOGIC MAP OF THE FUMAROLE BUTTE AREA JUAB AND MILLARD COUNTIES, UTAH

By J.B. Peterson
University of Utah (1978)

EXPLANATION



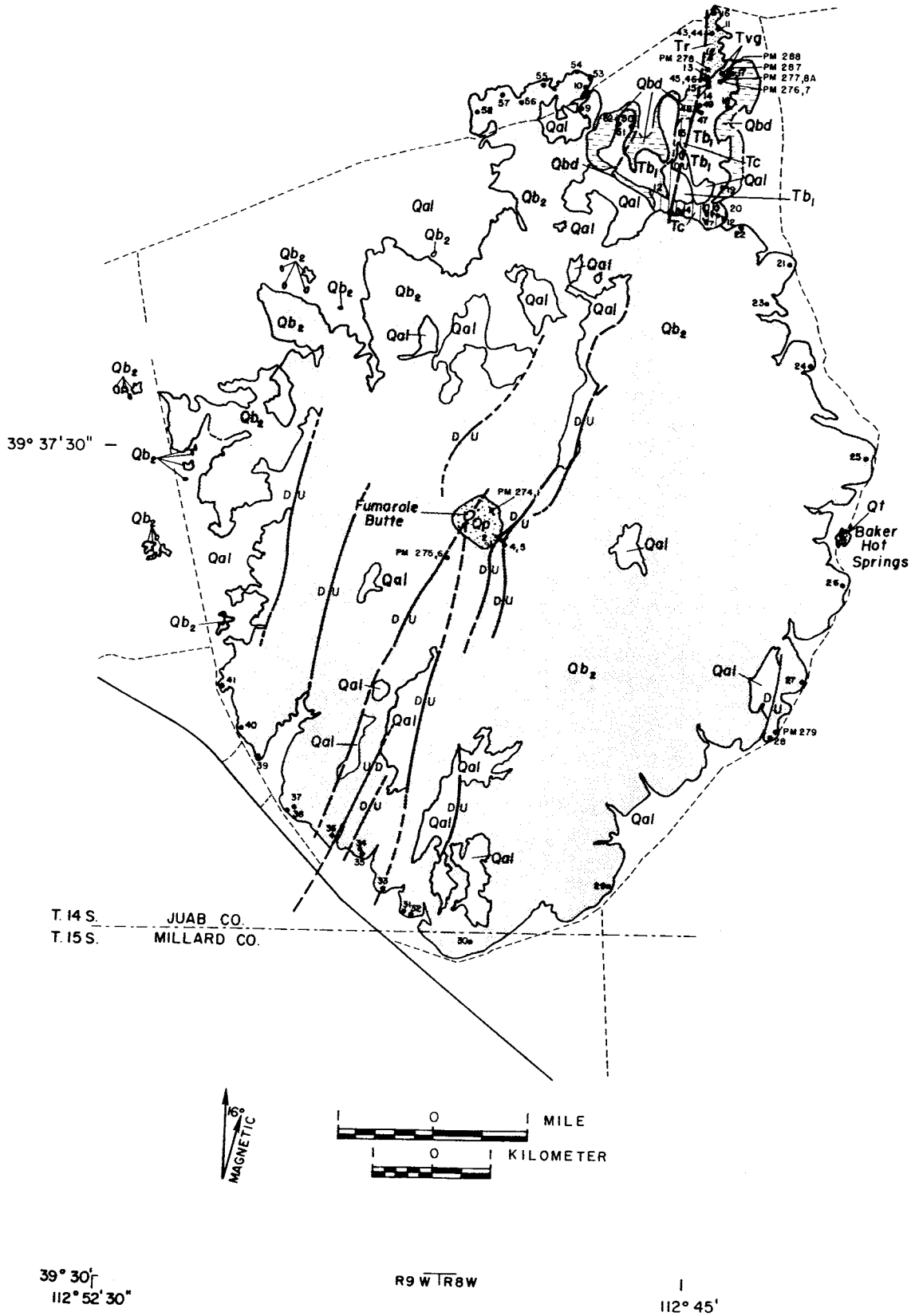


Figure 2. Geologic map of the Fumarole Butte volcanic complex.

area about 4,000 meters northeast of the volcanic neck. Johnson concluded that the basalt - sediment contact is nearly horizontal and that the difference in thickness is mainly due to variation in elevation between the two areas. He found anomalously high and low resistivity values in the area of the volcanic neck which he attributed to a localized fracture zone through which the basalt was extruded. Johnson concludes that Fumarole Butte is an isolated basalt flow overlying several hundred meters or more of lacustrine and fluvial sediments.

Both Fumarole Butte and North Butte are cut by several high-angle, normal faults. The faults are sub-parallel and most are oriented about N 25° E. Apparent displacement ranges from about 15 to 30 meters with most of the down dropped blocks lying to the west. Similar major faulting is present in the volcanic rocks of the Smelter Knolls area which lies 12 km to the south (Turley and Nash, 1980). The alignment and orientation of major faults in each area suggest that a fault system extends from Fumarole Butte to Smelter Knolls; however, a thick cover of alluvium between these areas conceals any evidence of faulting. A continuous fault system from Fumarole Butte to Smelter Knolls could reflect a significant structural discontinuity throughout this area, possibly related to a major structure as suggested by Smith (1974).

Crater Springs are located on the eastern margin of Fumarole Butte. Several springs produce hot water from a tufa mound that is about 5 meters high and several hundred meters in diameter. Mundorf (1970) reported that one spring had a temperature of 87°C in August, 1964, and again in July, 1967. Nash measured a temperature of 90°C in July, 1975. Mundorf (1970) estimated the discharge rate to be about 250 gpm in July, 1967.

GEOCHRONOLOGY

Ages were determined for the basaltic andesite, tholeiite, and rhyolite using standard K-Ar age dating techniques. Sanidine separates were used to determine the age of the rhyolite, whereas whole rock samples were used for the basaltic andesite and tholeiite. All samples were analyzed for potassium by flame photometry. The pertinent analytical data are listed in table 1.

Ages for representative samples of the Fumarole Butte volcanics were determined to be: basaltic andesite, 0.88 ± 0.1 m.y.; tholeiite, 6.03 ± 0.1 m.y.; and rhyolite, 6.18 ± 0.1 m. y. Basaltic andesite and tholeiite from the Smelter Knolls area have been dated at 6.11 ± 0.3 m.y.

and 0.31 ± 0.08 m.y., respectively (Turley and Nash, 1980). The contrasting ages of volcanic types between Fumarole Butte and Smelter Knolls indicate at least two eruptive episodes of each magma type throughout this area. The age of the rhyolite at Fumarole Butte is similar to that determined for the Thomas Range rhyolite 15 km to the north (6.0 m.y. by Armstrong, 1970).

Paleomagnetic data were gathered on the basaltic andesite, tholeiite, rhyolite, and obsidian at Fumarole Butte, and are presented in table 2. Paleomagnetic results are consistent with the K-Ar age dates determined in this study. The basaltic andesite has normal polarity and should be assigned to the *Jaramillo* event (McDougall, 1977). The tholeiite has reversed polarity, and probably belongs in epoch 6 of the polarity time scale. The rhyolite and obsidian have reversed polarity and also are placed in epoch 6.

PETROGRAPHY

The volcanic rocks of the Fumarole Butte area consist of obsidian, crystalline rhyolite, basaltic andesite, and tholeiitic basalt. Modes and sample locations of the analyzed rocks are presented in table 3.

The obsidian (sample 76-8A) is friable, being composed of interlocking pieces of glass. Flow banding is apparent in hand specimen but more difficult to detect in thin section. The sample has a vitrophyric texture and is composed of more than 79 percent glass. The groundmass is spherulitic. Anhedral phenocrysts of unzoned sanidine are present as are anhedral phenocrysts of quartz. Plagioclase phenocrysts are also present but quite rare. Iron-titanium oxides are present as is biotite. Minor amounts of sphene and zircon were identified, and one small grain of allanite was found. The obsidian appears fresh, and only biotite is slightly altered.

The crystalline rhyolite (sample 76-12) is devitrified and has lithophysoidal cavities that are usually lined with secondary silica. Devitrified glass makes up more than 80 percent of the volume and is composed of a dense intergrowth of quartz and alkali feldspar. The groundmass is spherulitic. Flow banding is apparent in both hand specimen and thin section. Generally, phenocrysts in the rhyolite consist of plagioclase, subhedral sanidine, and anhedral quartz. Modal analysis indicates the volumetric abundance of plagioclase, sanidine, and quartz phenocrysts is about 1 percent, 5 percent, and 11 percent, respectively. Biotite and iron-titanium oxides are also present as are minor amounts of sphene. A single hornblende phenocryst was found in thin section, and

Table 1. K-Ar Analytical Data and Ages

Area	Rock Type	Material used	% K	moles/gm $^{40}\text{Ar}_{\text{rad}} (\times 10^{-11})$	$\%^{40}\text{Ar}_{\text{atm}}$	Age ($\times 10^6$) years
Fumarole Butte	Basaltic andesite	Whole rock	1.91	0.294	93.2	0.88 ± 0.1
Fumarole Butte	Tholeiitic basalt	Whole rock	1.055	1.105	72.4	6.03 ± 0.3
Fumarole Butte	Rhyolite	Sanidine	8.42	9.042	23.2	6.18 ± 0.1
*Smelter Knoll	Tholeiitic basalt	Whole rock	0.725	0.0384	97.3	0.31 ± 0.08
Smelter Knoll	Basaltic andesite	Whole rock	1.99	2.113	85.7	6.11 ± 0.3
Smelter Knoll	Rhyolite	Sanidine	7.225	4.270	28.6	3.40 ± 0.1

*Analytical data and ages for samples from Smelter Knoll were supplied by Turley (1978).

Table 2. Paleomagnetic Data

Locality	Station	Rock Type	Demag.	D	I	N	K	a_{95}°	P
Fumarole Butte	274	basaltic andesite	100	27	63	4	531	3.9	N
Fumarole Butte	275	basaltic andesite	100	332	61	7	184	4.4	N
Fumarole Butte	276	tholeiitic basalt	200	131	-77	6	17	16.7	R
Fumarole Butte	277	obsidian	200	160	-56	6	30	12.3	R
Fumarole Butte	278	rhyolite	800	28	-74	7	149	4.9	I
Fumarole Butte	279	basaltic andesite	200	339	59	2	-	-	N
Fumarole Butte	287	tholeiitic basalt	NRM	158	-70	6	465	3.1	R
Fumarole Butte	288	obsidian	NRM	155	-61	8	151	4.5	R

Demag. = AF demagnetization field strength (oe).

D = declination; I = inclination; N = number of samples

K = Fischer coefficient; P = polarity (N, normal; R, reversed; I, indeterminate)

a_{95}° = half angle of cone of 95% confidence around mean direction

Table 3. Modal Analyses (volume percent)

Sample No.	76-8A	76-12	76-14	76-48	76-9	76-36
Quartz	6.1	11.0	-	0.2	-	0.1
Alkali feldspar	12.0	5.4	-	-	-	-
Plagioclase	1.7	0.8	25.5	18.3	39.1	40.4
Clinopyroxene	-	-	-	-	13.3	26.9
Olivine	-	-	8.2	10.5	-	-
Biotite	0.3	0.4	-	-	-	-
Amphibole	-	tr.	-	-	-	-
Orthopyroxene	-	-	-	-	-	tr.
Glass	79.8	-	-	-	-	-
Opagues	0.1	0.4	7.5	11.6	3.1	7.4
Groundmass (undifferentiated)	-	82.0	58.7	59.4	44.5	25.2

Key to Sample Localities

Sample No.	Sample Location	Rock Type
76-3	700 m southeast of volcanic neck	Basaltic andesite
76-8A	North end of North Butte	Obsidian
76-9	North end of Fumarole Butte flow	Basaltic andesite
76-12	North end of North Butte	Rhyolite
76-14	North end of North Butte flow	Tholeiite
76-36	Southwest side of Fumarole Butte flow	Basaltic andesite
76-48	North end of North Butte flow	Tholeiite

the wide reaction rim encircling the crystal indicates disequilibrium between hornblende and the melt. The crystalline rhyolite is more extensively altered than the obsidian, but alteration is moderate and most apparent around the margins of biotite grains.

Three samples of basaltic andesite were analyzed (76-3, 76-9, and 76-36). Sample 76-3 is fine grained, vesicular, and contains abundant, dark-brown volcanic glass. The two other samples are considerably coarser grained and less glassy. Phenocrysts are not common in the basaltic andesite; however, a quartz xenocryst was found in sample 76-36. The xenocryst is about 5 cm in diameter and is surrounded by reaction rims of brown glass and pyroxene. Best and Brimhall (1974) report quartz xenocrysts in basaltic andesite from southwestern Utah and consider them to be cognate in nature. Similar lavas have been described by Hausel and Nash (1976) who postulate that such quartz xenocrysts may have formed under mantle conditions from material parental to basaltic andesite.

The basaltic andesite has subophitic texture. The groundmass consists of plagioclase laths and subhedral pigeonite. Orthopyroxene is scarce in the basaltic andesite. The presence of orthopyroxene in all samples was sought with electron microprobe analysis, and only three relatively large groundmass crystals were found in sample 76-36. No orthopyroxene was found in samples 76-3 or 76-9. Iron-titanium oxides are present in the basaltic andesite and were twice as abundant in 76-36 as in 76-9. In general, the basaltic andesite is fresh with only minor alteration of pyroxene in sample 76-36.

Two samples of tholeiite (76-14 and 76-48) were analyzed. The groundmass is composed of laths of plagioclase, subhedral diopsidic augite, and subhedral olivine. Iron-titanium oxides are present as accessory minerals in both, but are somewhat more abundant in 76-48. Both samples are vesicular and calcite is commonly found coating the vesicles. The tholeiite contains abundant phenocrysts of plagioclase feldspar and subhedral to anhedral olivine. Alteration is more prominent in the tholeiite than the basaltic andesite. Olivine phenocrysts and groundmass olivine crystals show moderate alteration as do groundmass pyroxene crystals.

MINERALOGY

Minerals of the Fumarole Butte volcanics were analyzed with an ARL EMX-SM electron microprobe. Natural mineral standards were used, and Bence-Albee (1968) corrections for matrix effects were applied when

standards and samples differed appreciably in composition. If the composition of samples and standards were similar, the only correction applied was for background radiation.

Feldspar

Both alkali feldspar and plagioclase are present in the Fumarole Butte volcanics. Feldspar compositions are shown in figure 3 and feldspar analyses are presented in table 4.

Alkali feldspar occurs only in rhyolite. Feldspar phenocrysts range in orthoclase content from Or₆₀ to Or₆₈. Compositional zoning was not detected within individual phenocryst grains.

With the exception of the obsidian, plagioclase is present in all analyzed samples. The most calcic varieties (up to An₇₀) occur as phenocrysts in the tholeiitic basalt; the most sodic in the tholeiite occur as groundmass grains of An₃₇. Phenocrysts of plagioclase are absent in the basaltic andesite whose groundmass feldspar consists of sodic labradorite and andesine. Unzoned oligoclase occurs as phenocrysts in the rhyolite.

Minor elements display systematic behavior in feldspars. Barium contents are higher in alkali feldspar than in plagioclase (0.14-0.17 vs. 0.0-0.6% BaO) whereas iron, as Fe₂O₃, is less in feldspar from rhyolite (0.15-0.77%) than in plagioclase from basaltic rocks (0.83-1.04%).

Olivine

Olivine is present in the tholeiitic basalt (samples 76-14 and 76-48) where it occurs both as phenocrysts and in the groundmass. The compositional range is shown in figure 3. Analyses and structural formulas are presented in table 5. An extreme compositional range occurs in the olivine phenocrysts which vary from Fo₈₀ to Fo₅₀. Normal zoning is apparent in most phenocrysts with compositions generally changing about 13 percent from core to rim; however, strong zoning is present in some phenocrysts which vary in composition up to 30 percent. Groundmass olivine crystals are zoned with a compositional range from Fo₇₀ to Fo₃₉.

Pyroxene

Clinopyroxene is present as a groundmass phase in both the basaltic andesite and the tholeiite. In the tholeiite, clinopyroxene is diopsidic augite, whereas in

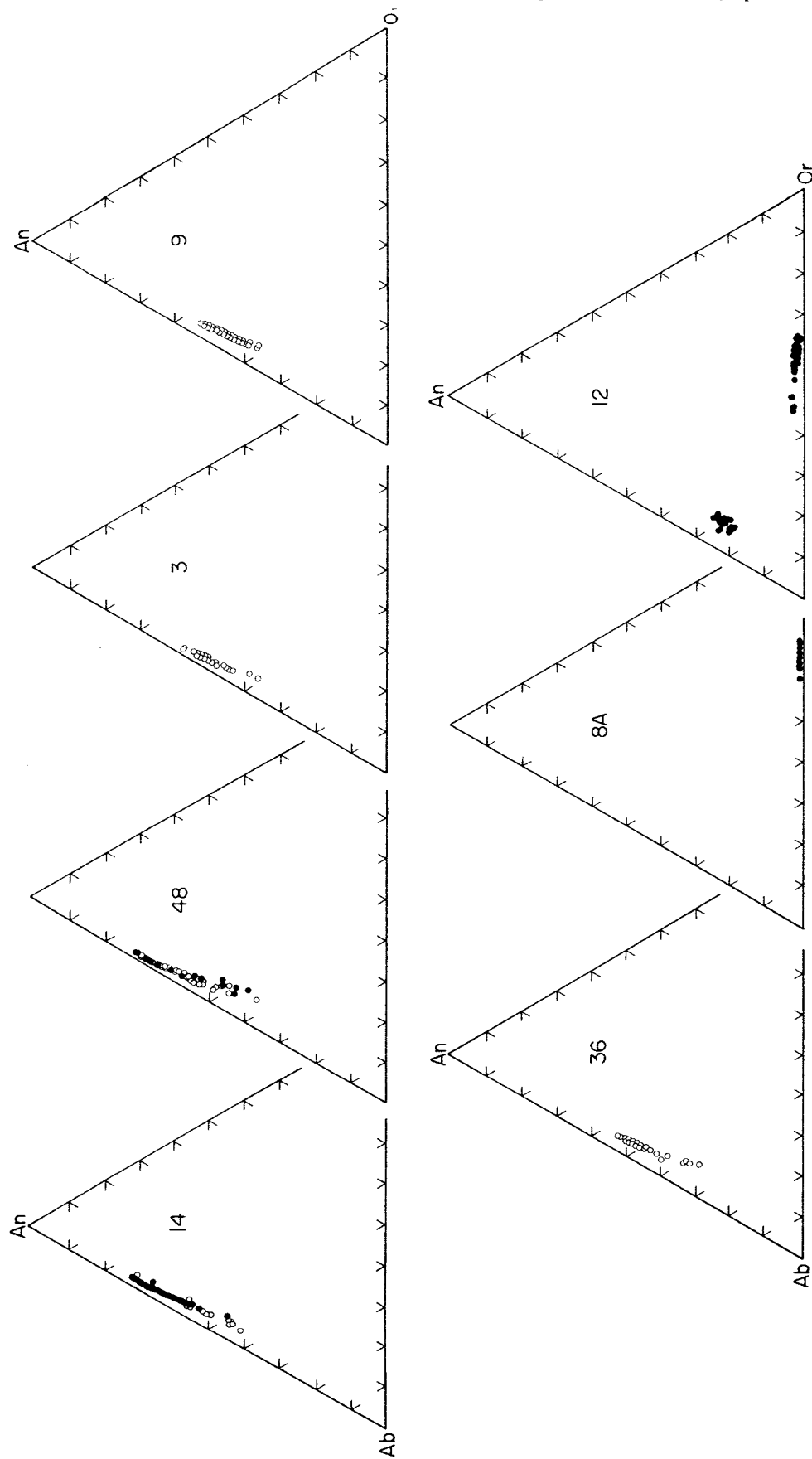


Figure 3. Microprobe analyses of feldspar from the Fumarole Butte Volcanic Complex in mole percent anorthite, albite, and orthoclase. Solid circles are phenocrysts, open circles are groundmass grains. For key to analyses see table 3.

Table 4. Average Microprobe Analyses of Feldspar p = phenocrysts; g = groundmass

Sample No.	Plagioclase Feldspars						Alkali Feldspars			
	76-12 (p)	76-3 (g)	76-9 (g)	76-36 (g)	76-14 (g)	76-14 (p)	76-48 (g)	76-48 (p)	76-8A (p)	76-12 (p)
Weight Percent										
CaO	4.53	10.2	9.74	9.69	13.0	13.3	12.5	13.1	0.30	0.40
Na ₂ O	8.13	5.50	5.64	5.64	3.93	3.77	4.17	3.82	3.69	4.71
K ₂ O	1.44	0.53	0.54	0.70	0.37	0.40	0.43	0.44	11.5	9.64
BaO	-	0.05	0.06	0.06	0.03	0.02	0.04	0.04	0.14	0.17
Fe ₂ O ₃ *	0.27	1.04	0.88	0.97	0.87	0.83	1.04	0.99	0.15	0.15
Weight Percent										
An	22.5	50.5	48.3	48.1	64.5	65.8	61.9	65.0	1.5	2.00
Ab	68.8	46.5	47.7	47.7	33.3	31.9	35.3	32.3	31.2	39.7
Or	8.5	3.2	3.2	4.2	2.2	2.3	2.6	2.6	67.7	56.7
Cn	-	0.1	0.2	0.2	0.1	0.1	0.1	0.1	0.3	0.4
Total	99.8	100.3	99.4	100.2	100.1	100.1	99.9	100.0	100.7	98.8
Recalculated Mole Percent										
An	21.5	49.0	47.3	46.8	63.3	64.5	60.7	63.8	1.5	2.0
Ab	70.3	47.9	49.6	49.2	34.6	33.2	36.8	33.7	32.4	41.6
Or	8.2	3.1	3.1	4.0	2.1	2.3	2.5	2.5	66.2	56.4

*Total iron reported as Fe₂O₃

Table 5. Average Microprobe Analyses and Structural Formulas of Olivines

p = phenocrysts; g = groundmass

Sample No.	76-14(g)	76-14(p)	76-48(g)	76-48(p)
SiO ₂	34.2	37.6	34.4	37.3
TiO ₂	0.11	-	0.12	-
Al ₂ O ₃	0.09	0.03	0.13	0.05
*FeO	37.8	22.1	38.3	21.4
MnO	0.63	0.28	0.61	0.26
NiO	-	-	-	-
MgO	25.5	38.2	25.0	39.2
CaO	0.47	0.43	0.46	0.40
TOTAL	98.8	98.6	99.0	98.6

Number of Atoms on the Basis of 4 oxygens

Si	0.98	0.99	0.99	0.98
Al	0.00	0.00	0.00	0.00
Ti	0.00	0.00	0.00	0.00
Fe ⁺²	0.91	0.49	0.92	0.47
Mn	0.02	0.01	0.02	0.01
Mg	1.09	1.51	1.07	1.54
Ca	0.01	0.01	0.01	0.01

[2.03] [2.02] [2.02] [2.03]

Weight Percent

Fo	44.5	66.7	43.6	68.4
Fa	53.6	31.3	54.4	30.3
Tp	0.9	0.40	0.9	0.4
La	0.7	0.7	0.7	0.6
TOTAL	99.7	99.1	99.6	99.7

Mole Percent

Fo	54.8	74.3	62.9	77.5
Fa	44.4	25.1	36.4	21.9

- : not detected

*Total iron reported as FeO

the basaltic andesite it is pigeonite (figure 4 and table 6).

Generally, the pyroxene composition is uniform within each volcanic group; however, some compositional differences do exist between groups. Pyroxenes of the basaltic andesite are enriched in Fe and Mg, and depleted in Ti and Ca relative to those in the tholeiite. Al and Na are considerably depleted in basaltic andesite pyroxenes as compared to pyroxenes in the tholeiite. Although pyroxene in the tholeiite contains more Na and Al than that in the basaltic andesite, Na and Al content of pyroxene in the tholeiite is low. Green and Ringwood (1968) suggest that this indicates crystallization at shallow depth.

Orthopyroxene occurs only as a few relatively large groundmass grains in the basaltic andesite. The orthopyroxene ranges in composition from Fs_{42} to Fs_{46} and contains 4.5 percent CaO.

Biotite

Biotite is a common accessory mineral in the silicic rocks. Microprobe analyses of biotite are presented in table 7; the low totals are attributed to the presence of water which cannot be detected with microprobe techniques.

Biotites from the obsidian and rhyolite are very similar in chemical composition. Mg content averages 13 percent and Fe about 17.5. The biotites are high in TiO_2 (3.5 percent), and contain substantial F. Biotites from the obsidian contain 3.00 percent F and those from the rhyolite an exceptional 6.59 percent.

Iron - Titanium Oxides

Iron - titanium oxides occur as microphenocrysts and/or in the groundmass in each of the Fumarole Butte volcanic rock types. Magnetite and ilmenite are common in obsidian, rhyolite, and tholeiite. Magnetite is also abundant in the basaltic andesite; however, ilmenite is rare and only a few grains were found.

Analyses of iron-titanium oxides are given in table 8. Of the minor elements, V, Mg, and Ca are higher in oxides from the tholeiite and basaltic andesite, whereas the concentration of Mn is higher in oxides from the obsidian and rhyolite. Generally, Fe, Al, Zn, Cr, and V are concentrated in magnetite, and Ti, Mn, and Mg are more abundant in ilmenite. The mole percent ulvospinel in titanomagnetite ranges from 29.5 in sample 76-8A to 79.3 in sample 76-36, and the R_2O_3 concentration in

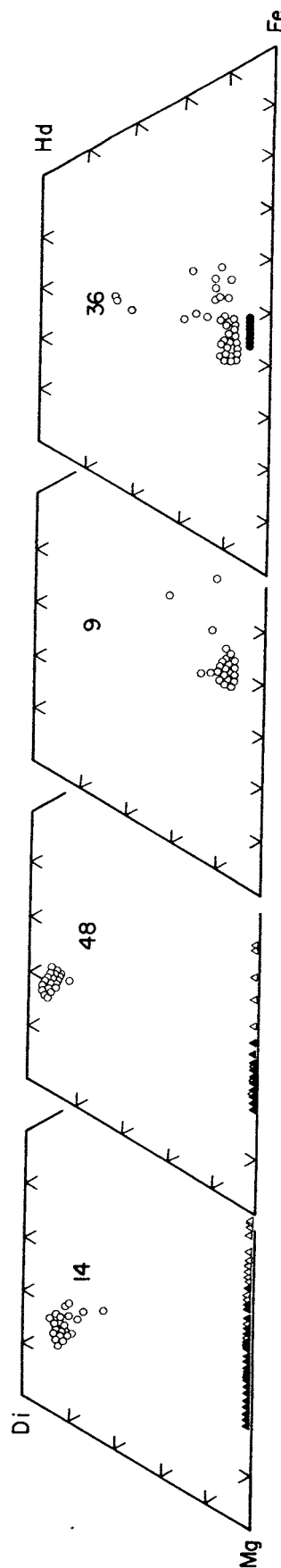


Figure 4. Microprobe analyses of pyroxene (circles) and olivine (triangles) from the Fumarole Butte volcanic complex. Solid symbols are phenocryst phases; open symbols are groundmass grains. For key to analyses see Table 3.

Table 7. Average Microprobe Analyses and Structural Formulas of Biotites

Sample No.	76-8A	76-12
SiO ₂	38.7	38.6
TiO ₂	3.64	3.46
Al ₂ O ₃	11.6	11.8
FeO*	17.5	17.7
MnO	0.28	0.55
MgO	13.6	12.8
CaO	0.07	0.09
Na ₂ O	0.52	0.55
K ₂ O	9.25	9.34
BaO	-	-
F	3.00	6.59
Cl	0.12	0.14
Sum	98.3	101.6
-O≡F, Cl	1.29	2.81
Total	97.0	98.8

Number of Atoms on the Basis of 22 Oxygens	
Si	5.87
Al	2.08
Ti	0.05
Al	-
Ti ⁺²	0.36
Fe	2.22
Mn	0.04
Mg	3.08
Ca	0.01
Na	0.15
K	1.79
Ba	0.00

- : not detected
*Total iron reported as FeO

Table 6. Average Microprobe Analyses and Structural Formulas of Clinopyroxenes.

Sample No.	76-9	76-36	76-14	76-48
SiO ₂	51.4	51.5	50.1	48.0
TiO ₂	0.51	-	1.12	2.16
Al ₂ O ₃	0.86	0.86	2.26	3.53
FeO*	24.5	26.0	11.1	12.8
MnO	0.60	0.28	0.30	0.27
MgO	18.0	17.0	14.5	11.9
CaO	3.7	3.95	19.8	21.1
Na ₂ O	0.14	0.04	0.29	0.38
Total	99.7	99.6	99.5	100.1

Recalc. Mole Percent

En	46.0	43.1	37.1	30.5
Fs	46.2	48.5	21.0	24.3
Wo	7.8	8.3	41.9	45.1

Number of Atoms on the Basis of 6 Oxygens

Si	1.97	1.98	1.90	1.83
Al	0.03	0.02	0.10	0.16
Ti	-	-	0.00	0.01
Al	0.00	0.02	-	-
Ti ⁺²	0.02	0.00	0.03	0.05
Fe	0.78	0.83	0.35	0.41
Mn	0.02	0.01	0.01	0.01
Mg	1.03	0.97	0.82	0.68
Ca	0.15	0.16	0.80	0.86
Na	0.01	0.00	0.02	0.03

- : not detected
*Total iron reported as FeO

Table 8. Average Microprobe Analyses of Iron Titanium Oxides
 T = Titanomagnetite; I = Ilmenite

Sample No.	76-8A		76-12		4A		76-9		76-36		76-14		76-48	
	T	I	T	I	T	I	T	I	T	I	T	I	T	I
SiO ₂	0.41	0.45	0.48	0.45	0.37	0.48	0.40	0.48	0.45	0.33	0.37	0.36	0.28	0.39
TiO ₂	10.4	49.0	11.7	49.0	26.5	50.2	22.5	49.0	27.2	49.0	19.4	47.9	16.2	45.4
Al ₂ O ₃	1.20	0.14	2.74	0.12	1.99	0.28	2.20	0.28	1.43	0.55	1.75	0.32	2.25	0.58
Cr ₂ O ₃	0.02	-	-	-	0.02	-	-	-	-	-	0.09	0.01	0.30	0.01
V ₂ O ₃	0.35	0.08	0.36	0.10	0.43	0.09	0.84	0.09	0.60	0.29	1.21	0.50	0.89	0.25
FeO	82.7	49.6	79.7	47.2	66.9	46.0	70.3	45.4	66.8	45.4	72.7	46.6	72.9	47.5
MnO	0.97	1.75	1.46	1.87	0.64	0.66	0.45	0.64	0.57	0.64	0.45	0.52	0.48	0.45
MgO	0.50	0.90	-	0.04	0.58	0.50	1.20	0.50	1.18	3.46	1.56	2.17	1.80	2.83
CaO	-	-	-	0.02	0.13	0.23	0.11	0.17	0.11	0.17	0.20	0.45	0.24	0.34
NiO	-	-	-	-	-	-	-	-	-	-	-	-	-	-
ZnO	0.10	0.06	0.13	-	0.30	-	0.12	0.13	0.12	0.13	0.16	0.10	0.16	0.10
Sum	96.7	102.0	96.6	98.8	97.9	98.4	98.2	99.9	98.5	99.9	97.9	98.9	95.6	97.9
Recalculated Iron														
Fe ₂ O ₃	48.7	11.2	43.8	4.39	15.2	44.6	22.4	15.1	7.99	29.9	8.09	34.4	13.0	
FeO	38.8	39.6	40.2	43.3	53.2	1.60	49.3	53.3	38.2	45.9	39.3	42.0	35.9	
Total	101.6	100.5	100.9	99.3	99.4	98.6	100.5	100.7	100.9	100.7	100.9	99.8	99.0	99.2
Mol% Ulvsp.	29.5		35.1		78.7		66.1		79.3		55.5		46.1	
Mol% R ₂ O ₃	12.5		5.41		2.64		9.91		9.91		9.75		15.0	
Temp.	805°C		750°C		965°C		1195		1195		980°C		990°C	
-log f _{O₂}	13.5		11.1		12.6		8.5		8.5		11.1		10.3	

Fe₂O₃ calculated using the method of Carmichael (1967), T and -log f_{O₂} were determined from the calibration curves of Buddington and Lindsley (1964).

- : not detected

ilmenite from 2.64 in sample 4A to 15.0 in sample 76-48.

CHEMISTRY

Major Elements

Chemical analyses and CIPW norms of selected samples are presented in table 9. In addition, electron microprobe analyses of residual glass from samples 76-8A (obsidian) and 76-3 (basaltic andesite) are given. Samples were analyzed using the chemical procedures described by Carmichael *et al.* (1968). Fluorine concentrations were determined colorimetrically by the lanthanum alizarine blue method as described by Hall and Walsh (1969).

The obsidian and rhyolite are rich in silica, containing about 74 to 77 percent, respectively. When recalculated on an anhydrous basis silica values from both rock types fall between 76 and 77 percent. Al, Ca, and Mg concentrations are low while the ratios of Fe to Mg and Ca to Mg are high. Similar compositions of siliceous volcanics in the Mineral Mountains of Utah have been described by Evans (1978), who notes that such characteristics may be unique to rhyolites of bimodal basalt-rhyolite provinces.

Normative corundum is found in samples 76-8A (obsidian) and 76-12 (rhyolite), and is attributed to the presence of fluorine in these samples. The whole rock chemistry of 76-8A obsidian and 76-12 (crystalline rhyolite) is very similar; however, fluorine content is appreciably higher in 76-8A than in 76-12. Similarly, Zielinski *et al.* (1977) determined that fluorine is depleted in most felsites relative to their obsidian counterparts. Although fluorine was lost from the crystalline rhyolite, biotite in this rock contains a considerable amount of fluorine. The loss of fluorine by the crystalline rhyolite was probably a magmatic process and not due to exchange with meteoric water which would have also extracted fluorine from biotite, as appears to be the case in the Skaergaard intrusion (Nash, 1976). Chlorine is also depleted in the crystalline rhyolite relative to the obsidian.

The basaltic andesite is quartz normative. SiO₂ content ranges from 55.28 to 55.87 weight percent. Total alkali concentrations vary from 5.48 to 5.91 percent and Al₂O₃ from 14.17 to 14.35 percent. Inspection of table 9 shows the chemical similarity of the analyzed samples of basaltic andesite.

Two samples of tholeiitic basalt were analyzed. In general, the tholeiite contains normative hypersthene, groundmass olivine, and calcic clinopyroxene; no calcium-poor pyroxene is present. Sample 76-48 is barely quartz normative and does not contain calcium-poor pyroxene. The tholeiite from the Fumarole Butte area is similar to the transitional tholeiites described by Best and Brimhall (1974) from the Grand Canyon area, which occupy a compositional range between tholeiites and alkali olivine basalts.

Residual glass is present in two samples and was analyzed with an electron microprobe (table 9). Relative to the whole rock, the glass is depleted in TiO₂, MgO, and total iron, as is expected because these elements should be concentrated in the crystalline material with respect to residual liquids.

The residual glass of sample 76-3 (basaltic andesite), when compared with the whole rock analysis, is depleted in Al₂O₃ and CaO which partition into feldspar and pyroxene, enriched in Na₂O and K₂O. The residual glass is relatively enriched in TiO₂ but depleted in total iron.

The low analytical totals in both samples reflect the high water content of the residual glass which cannot be detected with microprobe techniques.

Trace Elements

Trace element concentrations were obtained for 12 elements (table 10) with Li, Be, and Cl not sought in basalt and basaltic andesite. Li and Be concentrations were analyzed by atomic absorption spectrometry; all other elements were determined by X-ray fluorescence.

Table 10 illustrates that the three lava types are compositionally very distinct. With respect to the basalt, the basaltic andesite is relatively enriched in the incompatible elements Ba, Nb, Zr, Y, and Rb. The rhyolite is similar to other high silica alkalic lavas in the western U.S. These lavas are characterized by relatively low Ba, Sr and Zr, and significant concentrations of Li, Be, Nb, Rb, and Th (see for example Evans, 1978; Hildreth, 1977).

GEOBAROMETRY

An estimate of the pressure at which basaltic material is in equilibrium with its source (mantle material) may be obtained by a thermodynamic approach developed by Nicholls and Carmichael (1972) with

Table 9. Chemical Analyses and CIPW Norms of Volcanic Rocks and Residual Glasses.
For key to samples see Table 1.
G = microprobe analysis of glass.

Sample No.	76-8A	76-8A(G)	76-12	76-14	76-48	76-3	76-3(G)	76-9	76-36
SiO ₂	74.45	75.1	76.89	48.99	48.46	55.28	58.6	55.87	55.73
TiO ₂	0.20	0.08	0.23	2.21	2.28	2.06	2.48	2.11	2.06
Al ₂ O ₃	11.94	12.0	11.86	15.19	15.00	14.17	12.4	14.20	14.35
Fe ₂ O ₃	0.55	n.d.	0.87	2.05	3.22	2.15	n.d.	2.01	2.56
FeO	0.56	0.36	0.18	9.85	8.71	8.91	9.36	8.39	8.25
MnO	0.03	-	0.06	0.15	0.17	0.22	0.09	0.22	0.22
MgO	0.14	0.01	0.21	7.35	7.24	2.98	1.12	2.76	2.82
CaO	0.66	0.60	0.49	8.81	9.40	6.28	5.10	6.06	6.05
Na ₂ O	3.07	3.07	3.01	2.69	2.58	3.38	4.04	3.52	3.42
K ₂ O	5.50	5.07	5.66	1.27	0.91	2.10	3.27	2.39	2.29
P ₂ O ₅	0.01	n.d.	0.06	0.62	0.71	1.18	n.d.	1.08	1.18
CO ₂	0.05	n.d.	0.09	0.08	0.26	0.06	n.d.	0.08	0.05
F	0.22	0.15	0.05	n.d.	n.d.	n.d.	0.11	n.d.	n.d.
H ₂ O ⁺	1.98	n.d.	0.09	0.15	0.28	0.60	n.d.	0.64	0.36
H ₂ O ⁻	0.12	n.d.	-	0.04	0.08	0.10	n.d.	0.15	0.15
Sum	99.48	96.6	99.75	99.48	99.30	99.47	96.6	99.48	99.49
-O:F	0.09	0.08	0.02	-	-	-	0.06	-	-
Total	99.39	96.5	99.73	99.45	99.30	99.47	96.6	99.48	99.49
q	34.64	37.28	36.92	-	0.20	9.14	8.54	8.98	9.86
c	0.47	0.94	0.37	-	-	-	-	-	-
or	32.50	29.96	33.45	7.50	5.38	12.41	19.32	14.12	13.53
ab	25.98	25.31	25.47	22.76	21.83	28.60	33.74	29.79	28.94
an	1.29	1.88	1.12	25.62	26.66	17.29	6.28	15.89	17.04
di-wo	-	-	-	5.65	5.72	2.41	7.61	2.76	2.07
di-en	-	-	-	3.17	3.49	0.95	1.42	1.09	0.85
di-fs	-	-	-	2.25	1.91	1.49	6.77	1.70	1.22
hy-en	0.35	0.02	0.52	9.95	14.55	6.47	1.37	5.78	6.17
hy-fs	0.30	0.53	-	7.08	7.97	10.10	6.49	8.97	8.82
ol-fo	-	-	-	3.64	-	-	-	-	-
ol-fa	-	-	-	2.85	-	-	-	-	-
mt	0.80	-	0.11	2.97	4.67	3.12	-	2.91	3.71
il	0.38	0.15	0.44	4.20	4.33	3.91	4.71	4.01	3.91
hm	-	-	0.79	-	-	-	-	-	-
ap	0.02	-	0.14	1.47	1.68	2.79	-	2.56	2.79
fr	0.45	0.31	0.10	-	-	-	0.23	-	-
cc	0.11	-	0.20	0.18	0.59	0.14	-	0.18	0.11
rest	2.10	-	0.09	0.19	0.36	0.70	-	0.79	0.51
Total	99.39	96.38	99.73	99.48	99.35	99.54	96.48	99.53	99.55

-: not detected

n.d.: not determined

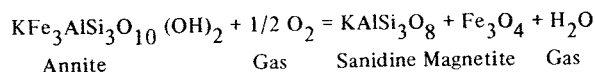
* Total iron in glasses reported as FeO

refinements given by Carmichael *et al.* (1977) and Nicholls (1977). A fundamental assumption of this method is that a magma forms in equilibrium with a mantle source and remains at constant chemical composition from source to surface. However, the mineralogy may and will certainly change due to varying pressure-temperature conditions.

The method is as follows: Chemical reactions between minerals and melt are formulated to define the activities of melt components contained in a specific sample. The activities of these components for surface conditions are estimated using groundmass mineral compositions and groundmass equilibration temperatures. Then the pressure at which a component is in equilibrium with the melt phase (for a specific reaction) is calculated as a function of temperature. Evaluation of each reaction over a temperature range produces a curve in P-T space that defines the activity of a specific component in the melt. When several reactions are evaluated, a family of curves is generated; ideally, the intersection of these curves represents the pressure and temperature conditions at which a magma was in equilibrium with its source material. These P-T conditions are assumed to represent the pressure and temperature regime from which a given sample of basaltic material was generated.

This method was applied to the tholeiitic basalt (samples 76-14 and 76-48) from the Fumarole Butte volcanics. (Unfortunately, it could not be applied to the basaltic andesite due to the limited mineral assemblage contained in this rock type). The reactions listed in table 11 are applicable to the minerals present in the tholeiite and were used to generate the corresponding activity curves shown in figure 5. The activity of components for surface conditions is determined using groundmass compositions of plagioclase, clinopyroxene, and olivine together with the Fe-Ti oxide temperature and oxygen fugacity for each sample. The activities of corresponding mantle materials were taken from Carmichael *et al.* (1977). Examination of figure 5 indicates that only one reasonable intersection is obtained for each sample. In each case the intersection of curves 3 and 5 at 18 kb to 19 kb and 1350°C to 1360°C possibly represents reasonable equilibration conditions. Unfortunately, no other intersections occur in P-T space representative of upper mantle conditions. Such results indicate that the preliminary assumption of unchanged composition from the source region is probably violated, and that re-equilibration and/or change in chemical composition has occurred in samples 76-14 and 76-48 since magma generation. The lack of a singular solution is good evidence that the tholeiitic lava does not represent pristine mantle material.

The depth at which siliceous volcanic rocks were equilibrated may be estimated from the fugacity of water in a magma, an approximation of which may be obtained from the following reaction (Wones and Eugster, 1965; Wones, 1972):



so that

$$\log f_{\text{H}_2\text{O}} = \frac{8673}{T} + 2.46 + 1/2 \log f_{\text{O}_2} + 3 \log X_{\text{Fe}^{2+}}^{\text{bio}} + 2 \log X_{\text{OH}^-}^{\text{bio}} - \log a_{\text{san}} = \log a_{\text{mt}}$$

The free energy function is that proposed by Hildreth (1977) and is based upon a reevaluation of the original experimental data of Wones and Eugster (1965). Temperatures and oxygen fugacities were provided by data previously determined from coexisting oxides. The OH⁻ term takes into account the effect of F substitution into the OH⁻ site in biotite (Ewart *et al.*, 1975). Sanidine activities are taken from Carmichael *et al.* figure 4-30; 1974, whereas magnetite activity is assumed to be equivalent to mole fraction, and annite activity is the cube of the mole fraction annite (Wones, 1972).

To estimate the minimum depth to pre-eruptive magma chambers, the following assumptions and approximations have been applied. Conversion of water fugacity to water pressure was done through interpolation of the data of Burnham *et al.* (1969). Hydrostatic pressure is assumed to be equal to lithostatic pressure. A conversion factor of 1 Kbar pressure = 3.83 Km lithospheric depth is used assuming an average crustal specific gravity of 2.7.

The application of this procedure of samples 76-8A (obsidian) and 76-12 (rhyolite) produces solutions of 1.08 km and .02 km, respectively. These are minimum depths because $f_{\text{H}_2\text{O}}$ could be less than hydrostatic pressure.

GEOOTHERMOMETRY

Various geothermometers were applied to the Fumarole Butte volcanics to determine groundmass crystallization temperatures and equilibration temperatures between phenocrysts and the melt phase (table 12). Application of geothermometry is restricted due to limited mineral assemblages in the Fumarole Butte volcanics.

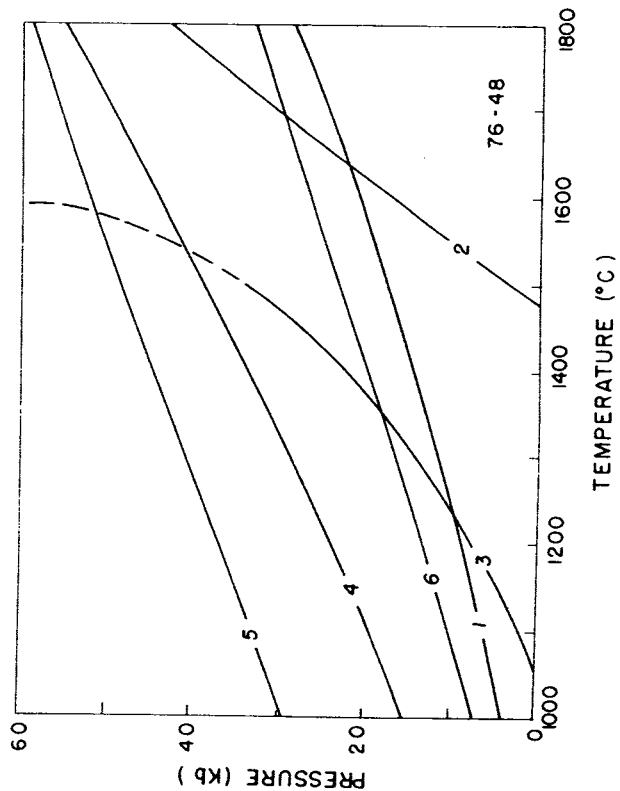
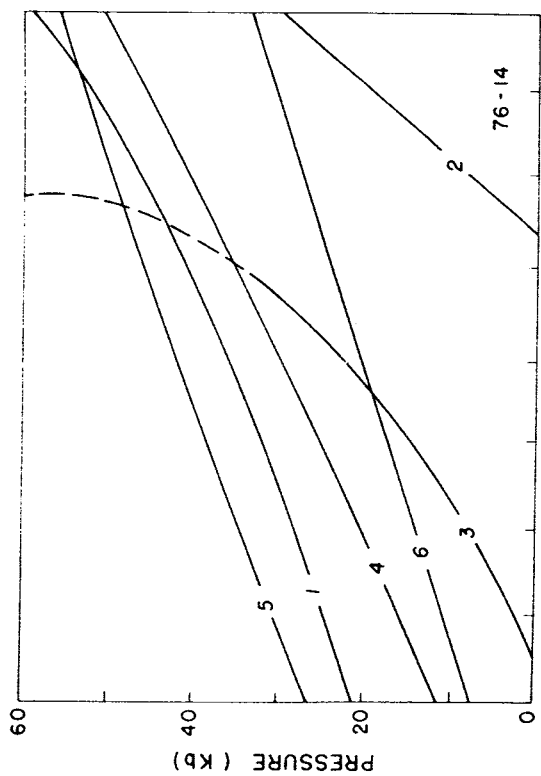


Table 10. Trace Element Analyses (XRF values rounded to nearest 5 ppm)

Sample No.	76-14	76-48	76-3	76-9	76-36	76-8A	76-12
Li	n.d.	n.d.	n.d.	n.d.	n.d.	31	43
Be	n.d.	n.d.	n.d.	n.d.	n.d.	6	7
Ba	840	860	1260	1280	1260	60	60
Nb	25	25	30	30	30	50	50
Zr	215	220	340	330	340	180	165
Y	30	30	50	50	45	50	45
Sr	460	465	450	435	435	30	30
Rb	25	20	40	45	45	330	335
Th	10	15	5	10	10	45	50
Pb	10	10	15	15	10	30	35
Zn	95	100	130	125	120	30	25
Cl	n.d.	n.d.	n.d.	n.d.	n.d.	520	40

n.d.: not determined

Figure 5. Calculated curves for equilibration of magma components (table 12) with model mantle material.

Table 11. Reactions used to define the activities of components in silicate melts.

No.	Reaction	Component
1	$\text{Mg}_2\text{SiO}_4 + \text{SiO}_2 = \text{Mg}_2\text{Si}_2\text{O}_6$ Olivine Melt Orthopyroxene	SiO ₂
2	$\text{Fe}_2\text{SiO}_4 = \text{Fe}_2\text{SiO}_4$ Melt Olivine	Fe ₂ SiO ₄
3	$\text{CaMgSi}_2\text{O}_6 = \text{CaMgSi}_2\text{O}_6$ Melt Clinopyroxene	CaMgSi ₂ O ₆
4	$\text{Mg}_2\text{SiO}_4 + \text{Al}_2\text{O}_3 = 1/2 \text{Mg}_2\text{Si}_2\text{O}_6 + \text{MgAl}_2\text{O}_4$ Olivine Melt Orthopyroxene Spinel	Al ₂ O ₃
5	$3\text{CaMgSi}_2\text{O}_6 + \text{Al}_2\text{O}_3 = \text{Ca}_3\text{Al}_2\text{Si}_3\text{O}_{12} + 3/2 \text{Mg}_2\text{Si}_2\text{O}_6$ Clinopyroxene Melt Grossular Orthopyroxene	Al ₂ O ₃
6	$\text{NaAlSi}_3\text{O}_8 + \text{Mg}_2\text{SiO}_4 = \text{Mg}_2\text{Si}_2\text{O}_6 + \text{NaAlSi}_2\text{O}_6$ Melt Olivine Orthopyroxene Clinopyroxene	NaAlSi ₃ O ₈

Table 12. Geothermometry

Sample No.	76-8A	76-12	76-3	4A	76-9	76-36	76-14	76-48
Iron-Titanium Oxides	905°C	750°C	-	965°C	-	1195°C	980°C	990°C
Two Feldspar (100 bars)	-	784°C	-	-	-	-	-	-
Clinopyroxene-Olivine	-	-	-	-	-	-	1025°C	1024°C
Kudo Weill core temp. (1kbar)	-	873°C	1029°C	-	1020°C	1018°C	1154°C	1137°C
Kudo-Weill rim temp. (1kbar)	-	-	1102°C	-	1088°C	1084°C	1203°C	1191°C
Revised Kudo-Weill core temp. (1kbar)	-	-	1017°C	-	1003°C	999°C	1120°C	1110°C
Revised Kudo-Weill rim temp. (1kbar)	-	810°C	1044°C	-	1034°C	1031°C	1192°C	1171°C
Revised Kudo-Weill core temp. (1 bar)	-	-	1081°C	-	1069°C	1066°C	1169°C	1160°C
Revised Kudo-Weill rim temp. (1 kbar)	-	-	1029°C	-	1012°C	1008°C	1152°C	1140°C

Coexisting Fe-Ti oxides were found in basaltic andesite samples 76-36 and 4A. The temperatures and oxygen fugacity determined for 76-36 appear unreasonably high (1195°C and $10^{-8.5}$), while those from section 4A are 965°C and $10^{-12.6}$, which are more reasonable. Oxides from the tholeiite produce equilibration temperatures of 980 to 990°C and oxygen fugacities of $10^{-11.1}$ and $10^{-10.3}$. The obsidian temperature and oxygen fugacity is about 805°C and $10^{13.5}$, and the crystalline rhyolite about 750°C and $10^{-11.1}$.

The olivine-clinopyroxene thermometer developed by Powell and Powell (1974) was applied to groundmass olivine and pyroxene in the tholeiite at 1 bar pressure. Sample 76-14 produced a temperature of 1025°C and sample 76-48 a temperature of 1024°C. These temperatures agree reasonably well with those determined from coexisting iron-titanium-oxides.

The two-feldspar thermometer developed by Stormer (1975) was applied to sample 76-12 (rhyolite). Temperature was calculated at 100 bars pressure using the average composition of alkali feldspar and plagioclase phenocrysts (no zoning was detected through microprobe examination of alkali feldspar and plagioclase phenocrysts in this sample). A temperature of 784°C was obtained, which records the temperature at which feldspar phenocrysts would be in equilibrium. Agreement between the two-feldspar and iron-titanium-oxide thermometers is good.

The plagioclase thermometer of Kudo and Weill (1970) and the revised version by Mathez (1973) were applied to all Fumarole Butte rock types except 76-8A (obsidian). The results are tabulated in table 11. In all cases the Kudo-Weill and Mathez thermometers produce temperatures that are considerably higher than those obtained from other thermometers. The plagioclase thermometers give temperatures about 200°C higher for the rhyolite (76-12) than the two-feldspar thermometer, about 125°C higher for the basaltic andesite, and 200°C higher for the tholeiite than those derived from the Fe-Ti oxide thermometer.

PETROGENESIS

The Fumarole Butte volcanic complex is located along the eastern margin of the Basin and Range province, throughout which episodic volcanism has occurred over the past 30 million years. The Basin and Range is characterized by high heat flow, a relatively thin continental crust, and abnormally low seismic velocities in the underlying mantle. Although heat flow is highly

erratic throughout this province, mean heat flow for the Basin and Range is about twice that of stable continental areas (Lachenbruch and Sass, 1978). Seismic studies indicate that the average crustal thickness for this region is about 35 km; however, "subprovinces" with anomalously shallow (15 to 20 km) low shear velocities appear to be present (Priestley and Brune, 1978). One explanation of high heat flow and anomalously low, shallow shear velocities occurring sporadically throughout the Basin and Range is the upwelling of mantle material into the crust. In effect, the influx of mantle material to within 15 to 20 km of the surface would locally increase heat flow and could induce melting of lower crustal material.

Unfortunately, the limited mineral assemblage present in the basaltic andesite does not permit estimation of the pressure at which this material formed. Also, the pressure-temperature equilibration curves generated from mineral compositions in the tholeiite produce inconclusive results regarding the depth to generation of this magma. Therefore, the following discussion is generally theoretical.

The low Na₂O and Al₂O₃ concentrations in clinopyroxene from the Fumarole Butte tholeiite and basaltic andesite indicate that these materials may have undergone crystallization at shallow depths (Green and Ringwood, 1968). This interpretation is supported by the spatial arrangement of equilibration curves for samples 76-14 and 76-48 (figure 5). The absence of convergence in P-T space indicates that equilibrium at constant composition was not maintained for the tholeiite throughout its magmatic evolution. The experiments of Green and Ringwood (1967, 1968) indicate that magmas similar in composition to the tholeiite underwent fractional crystallization in deep crustal environments (15 to 35 km), and that the basaltic andesite may have been produced by partial melting of mantle material and subsequent fractional crystallization at depths less than 35 km. Quartz xenocrysts present in the basaltic andesite may represent high pressure cognate material that has undergone partial low-pressure resorption at shallow depths.

Pressure estimates determined from water fugacities indicate that the rhyolite and obsidian at Fumarole Butte were erupted from depths of at least 1 km. The age of the rhyolite corresponds with the age of the Thomas Range rhyolite and was probably generated from the same thermal event responsible for the extensive siliceous volcanism in the Thomas Range.

The fault system at Fumarole Butte probably reflects a zone of weakness in the crust through which the associated volcanics were extruded. The fault system appears to extend at least 10 km south to the Smelter Knolls volcanic area. Possibly the fault system at Fumarole Butte may be linked to extensive faulting and associated Cenozoic volcanism that occurs throughout areas to the south (e.g. the Black Rock Desert).

GEOHERMAL POTENTIAL

The volcanic rocks at Fumarole Butte are represented by two age groups. The tholeiite and rhyolite are approximately 6 m.y. old, whereas the younger, more extensive basaltic andesite was erupted at 0.88 ± 0.1 m.y. Late Cenozoic volcanism throughout the Basin and Range is characterized by this bimodal assemblage of basalt and high-silica rhyolite. As opposed to basalts, silicic magmas may have substantial residence times in the upper crust. Therefore, rhyolitic systems provide an attractive initial target for geothermal exploration, whereas systems composed entirely of basaltic material are less desirable. However, because the last rhyolite eruption took place 6 million years ago, it is very unlikely that silicic igneous activity is contributing to the geothermal potential of the area today.

The power loss of the thermal springs at Fumarole Butte, calculated from the flowrate of 1,000 l/min and a surface temperature of 90°C , is approximately 5.6 MW. Chapman and Wilson (personal communication) have observed that 30 to 50% of the heat flow in a given area could be absorbed by recharging groundwater. Assuming a normal Basin and Range heat flow of 80 mW/m^2 , the power loss of the springs can be accounted for by a recharge area of 230 to 140 km^2 , respectively. The annual discharge of the springs is approximately $5.3 \times 10^5 \text{ m}^3/\text{yr}$. Annual precipitation of 20 cm/yr (8 in.) over the areas above would provide 4.6×10^7 to $2.8 \times 10^7 \text{ m}^3/\text{yr}$ of water; i.e., an amount more than sufficient to account for the discharge.

Parry and Cleary (1978) determined a Na-K-Ca temperature of 155°C and a silica temperature of 110°C for the thermal spring. A temperature of 150°C would be attained in a normal Basin and Range geothermal gradient of $30^{\circ}\text{C}/\text{km}$ at depths of about 5 km. Parry and Cleary (1978) calculated mixing models for this spring, and concluded that the waters are the result of mixing approximately 50% of cold water with 50% thermal water of about 145°C temperature, in general agreement with the Na-K-Ca temperature. Because both the mass and thermal outputs of the springs can

be accounted for by local heat flow and precipitation, we suggest that the simplest explanation for the thermal springs is the heating of meteoric groundwater at depth by the regional geothermal gradient and not by a cooling igneous body at depth. Although the presence of nearly boiling water is attractive from a geothermal viewpoint, if the water is heated by circulation along deep fracture systems, drilling may produce isothermal results to considerable depth.

In summary, although silicic volcanism has occurred in the Fumarole Butte area, its age (6.0 m.y.) indicates that the geothermal potential associated with this phase of volcanism is low. The basaltic andesite shield volcano is much younger (0.9 m.y.); however, there is no evidence for a large magma chamber in the upper crust. Crater Springs lack evidence of very hot water at depth, and appear to have very limited geothermal potential for electrical power production. The attractiveness of the direct heat utilization of these warm waters is significantly diminished by the absence of habitation in this desolate desert region.

ACKNOWLEDGMENTS

This research was supported by U. S. Geological Survey grant 14-08-0001-G-343 and by the Mineral Leasing Fund of the University of Utah. Age dates were provided by F. H. Brown; C. H. Turley and S. H. Evans, Jr. assisted in the chemical analyses of the rocks.

REFERENCES

- Albee, A. L. and L. Ray, 1970, Correction factors for electron probe microanalysis of silicates, oxides, carbonates, phosphates and sulfates: *Anal. Chem.*, v. 42, no. 12, p. 1408-1414.
- Armstrong, R. L., 1970, Geochronology of Tertiary igneous rocks, eastern Basin and Range province, western Utah, eastern Nevada, and vicinity, U. S. A.: *Geochim. Cosmochim. Acta*, v. 34, p. 202-232.
- Atwater, T., 1970, Implications of plate tectonics for the Cenozoic tectonic evolution of western North America: *Geol. Soc. Amer. Bull.*, v. 81, p. 3513-3536.
- Bence, A. E. and A. L. Albee, 1968, Empirical correction factors for the electron microanalysis of silicates and oxides: *Jour. Geol.*, v. 76, p. 382-403.
- Best, M. G. and W. H. Brimhall, 1974, Late Cenozoic alkalic basaltic magmas in the western Colorado Plateau and the Basin and Range transition zone, U. S. A., and their bearing on mantle dynamics: *Geol. Soc. Amer. Bull.*, v. 85, p. 1677-1690.

- Buddington, A. F. and D. H. Lindsley, 1964, Iron-titanium oxide minerals and synthetic equivalents: *Jour. Petrol.*, v. 5, p. 310-357.
- Burnham, C. W., J. R. Holloway, and N.F. Davis, 1969, Thermodynamic properties of water to 1,000°C and 10,000 bars: *Geol. Soc. Amer. Sp. Paper* 132, 96 p.
- Carmichael, I. S. E., 1963, The crystallization of feldspar in volcanic acid liquids: *Quart. Jour. Geol. Soc. Lond.*, v. 119, p. 95-131.
- Carmichael, I. S. E., 1964, The petrology of Thingmuli, a Tertiary volcano in eastern Iceland: *Jour. Petrol.*, v. 5, p. 435-460.
- Carmichael, I. S. E., 1967, The iron-titanium oxides of salic volcanic rocks and their associated ferromagnesian silicates: *Contr. Mineral. Petrol.*, v. 14, p. 36-64.
- Carmichael, I. S. E., J. Hample, and R.N. Jack, 1968, Analytical data on the U. S. G. S. standard rocks: *Chem. Geol.*, 3, 59-64.
- Carmichael, I. S. E. and J. Nicholls, 1967, Iron-titanium oxides and oxygen fugacities in volcanic rocks: *Jour. Geophys. Res.*, v. 72, p. 4665-4687.
- Carmichael, I. S. E., J. Nicholls, F. J. Spera, B. J. Wood, and S. A. Nelson, 1977, High temperature properties of silicate liquids: Applications to the equilibration and ascent of basic magma: *Trans. Royal Soc. Lon., Series A* 286, p. 373-431.
- Carmichael, I. S. E., F. J. Turner, and J. Verhoogen, 1974, *Igneous petrology*: McGraw-Hill, Inc., New York, 739 p.
- Christiansen, R. L. and P. W. Lipman, 1972, Cenozoic volcanism and plate-tectonic evolution of the western United States. II. Late Cenozoic: *Phil. Trans. Royal Soc. London*, v. 271, p. 249-284.
- Condie, K. C. and C. K. Barsky, 1972, Origin of Quaternary basalts from the Black Rock desert region, Utah: *Geol. Soc. Amer. Bull.*, v. 83, p. 333-352.
- Deer, W. A., R. A. Howie, and J. Zussman, 1963, *Rock-forming minerals. Vol. 2 Chain silicates*: John Wiley and Sons, Inc., New York, 379 p.
- Deer, W. A., R. A. Howie, and J. Zussman, 1963, *Rock-forming minerals. Vol. 4 Framework silicates*: John Wiley and Sons, Inc., New York, 435 p.
- Ellis, A. J. and W. H. J. Mahon, 1963, Natural hydrothermal systems and experimental hot water/rock interactions: *Geochim. Cosmochim. Acta.* v. 27, p. 1323-1357.
- Ellis, A. J. and W. H. J. Mahon, 1967, Natural hydrothermal systems and experimental hot water/rock interactions (Part II): *Geochim. Cosmochim. Acta.* v. 31, p. 519-538.
- Erickson, M. P., 1963, Volcanic geology of western Juab County, Utah: *in* Utah Geological Society Guidebook to the Geology of Utah, no. 17. Beryllium and uranium mineralization in western Juab County, Utah, B. J. Sharp, and N. C. Williams, ed., p. 23-35.
- Evans, S. H., 1978, *Studies in Basin and Range volcanism*: Ph. D. Thesis, Univ. of Utah, 119 p.
- Ewart, A., W. Hildreth, and I. S. E. Carmichael, 1975, Quaternary acid magma in New Zealand: *Contr. Mineral. Petrol.*, v. 51, p. 1-27.
- Fournier, R. O. and A. H. Truesdell, 1973, An empirical Na-K-Ca geothermometer for natural waters: *Geochim. Cosmochim. Acta.* v. 37, p. 1255-1275.
- Gilbert, G. K., 1874, Preliminary geological report, expedition of 1872: U. S. Geol. Survey, West of 100th Meridian Proj. Rep. (Wheeler), p. 48-52.
- Gilbert, G. K., 1890, *Lake Bonneville*: U. S. Geol. Survey Monograph 1.
- Gilluly, J., 1928, Basin-Range faulting along the Oquirrh Range, Utah: *Geol. Soc. Amer. Bull.*, v. 39, p. 1103-1130.
- Gilluly, J., 1963, The tectonic evolution of the western United States: *Quart. Jour. Geol. Soc. Lond.*, v. 119, p. 133-174.
- Green, D. H., 1969, The origin of basaltic and nephelinitic magmas in the earth's mantle: *Tectonophysics*, v. 7, p. 409-422.
- Green, D. H., 1970a, A review of experimental evidence on the origin of basaltic and nephelinitic magmas: *Phys. Earth planet. Interiors*, v. 3, p. 221-235.
- Green, D. H., 1970b, The origin of basaltic and nephelinitic magmas: *Trans. Leicester Lit. Phil. Soc.*, v. 44, p. 26-54.
- Green, D. H. and A. E. Ringwood, 1967, The genesis of basaltic magmas: *Contr. Mineral. Petrol.*, v. 15, p. 103-190.
- Green, D. H. and A. E. Ringwood, 1968, Genesis of the calc-alkaline igneous rock suite: *Contr. Mineral. Petrol.*, v. 18, p. 105-162.
- Hall, A. and J. N. Walsh, 1969, Fluorine determination in rocks and minerals: *in* Laboratory Handbook of Petrographic Techniques, Hutchison, C. S., auth., John Wiley and Son Inc., New York, p. 272-273.
- Hamilton, W. and W. B. Meyers, 1966, Cenozoic tectonics of the western United States: *Rev. Geophys.*, v. 4, p. 509-549.
- Hausel, W. D. and W. P. Nash, 1976, Petrology of Tertiary and Quaternary volcanics from southwestern Utah: *Geol. Soc. Amer. Bull.*, v. 88, p. 1831-1842.
- Hildreth, E. W., 1977, The magma chamber of the Bishop Tuff: Gradients in temperature, pressure, and composition: Ph. D. Thesis, Univ. of Calif., Berkeley, 328 p.
- Hogg, N. C., 1972, Shoshonitic lavas in west central Utah:

- Brigham Young University Geology Studies, v. 19, part 2, p. 133-184.
- Irving, A. J. and D. H. Green, 1976, Geochemistry and petrogenesis of the Newer Basalts of Victoria and South Australia: *Journal Geology Society Australia*, volume 23, p. 45-66.
- Johnson, E. H., 1975, Resistivity and induced polarization survey of a basalt flow in a geothermal environment, western Utah: unpublished M. S. thesis, University of Utah, 69 p.
- Kudo, A. M. and D. F. Weill, 1970, An igneous plagioclase thermometer: *Contr. Mineral. Petrol.*, v. 25, p. 52-65.
- Lachenbruch, A. H. and J. H. Sass, 1977, Heat flow in the United States and the thermal regime of the crust *in* J. G. Heacock, ed., *The Earth's crust - its nature and physical properties*: *Amer. Geophys. Un. Mono.* 20, p. 626-678.
- Lipman, P. W., H. J. Prostka, and R. L. Christiansen, 1972, Cenozoic volcanism and plate-tectonic evolution of the western United States. I. Early and middle Cenozoic: *Phil. Trans. Royal Soc., London*, v. 271, p. 217-248.
- Mathez, E. A., 1973, Refinement of the Kudo-Weill plagioclase thermometer and its application to basaltic rocks: *Contr. Mineral. Petrol.*, v. 41, p. 61-72.
- McDougall, I., 1977, The present status of the geomagnetic polarity time scale: *Australian Nat. Univ. Res. School Earth Sci.*, Pub. No. 1288, 34 p.
- McKee, E. H., 1971, Tertiary igneous chronology of the Great Basin of western United States - implication for tectonic models: *Geol. Soc. Amer. Bull.*, v. 82, p. 3497-3502.
- Mundorff, J. C., 1970, Major thermal springs of Utah: *Utah Geological and Mineral Survey Water Res. Bull.* 13, 60 p.
- Nash, W. P., 1976, Fluorine, chlorine, and OH-bearing minerals in the Skaergaard intrusion: *American Journal Science*, v. 276, p. 546-557.
- Nash, W. P., I. S. E. Carmichael, and R. W. Johnson, 1969, The mineralogy and petrology of Mount Suswa, Kenya: *Journal Petrology* p. 409-439.
- Nash, W. P., C. Turley, J. Peterson and F. H. Brown, 1978, Volcanism and the regional assessment of geothermal resources in west-central Utah: *Geothermal Resource Council, Trans.*, v. 2, 475-477.
- Nash, W. P. and J. F. G. Wilkinson, 1970, Shonkin Sag Laccolith, Montana: I. mafic minerals and estimates of temperature, pressure, oxygen fugacity and silica activity: *Contr. Mineral. Petrol.*, v. 33, p. 162-170.
- Nicholls, J., 1977, The activities of components in natural silicate melts: *in* *Thermodynamics in Geology*, D. G. Fraser, ed., D. Reidel Publishing Company, Holland, p. 327-349.
- Nicholls, J. and I. S. E., Carmichael, 1972, The equilibration temperature and pressure of various lava types with spinel and garnet-peridotite: *American Mineral.*, v. 57, p. 941-959.
- Nicholls, J., I. S. E. Carmichael, and J. C. Stormer, 1971, Silica activity and P_{total} in igneous rocks: *Contr. Mineral. Petrol.*, v. 33, p. 1-20.
- Noble, D. C., V. C. Smith, and L. C. Peck, 1967, Loss of halogens from crystallized and glassy silicic volcanic rocks: *Geochim. Cosmochim. Acta*, v. 31, p. 215-223.
- Pakiser, L. C., 1965, The basalt-eclogite transformation and crustal structure in the western United States: *U. S. Geol. Survey Prof. Paper* 525B, p. B1-B8.
- Parry, W. T., N. L. Benson, and C. D. Miller, 1976, Geochemistry and hydrothermal alteration at selected Utah hot springs: *National Science Foundation Report*, contract GI-43741, Department of Geology and Geophysics, University of Utah, 131 p.
- Parry, W. T. and M. Clearly, 1978, Na-K-Ca and SiO_2 temperature estimates for Utah spring and well waters: *U. S. Geol. Surv. Rept.*, contract 14-08-0001-G-341, Dept. Geology & Geophysics, University of Utah, 51 p.
- Powell, M. and R. Powell, 1974, An olivine-clinopyroxene geothermometer: *Contr. Mineral. Petrol.*, v. 48, 249-263.
- Priestley, K. and J. Brune, 1978, Surface waves and the structure of the Great Basin of Nevada and western Utah: *J. Geophys. Res.*, 83, p. 2265-2272.
- Ringwood, A. E., 1975, *Composition and petrology of the earth's mantle*: McGraw-Hill, Inc., New York, 618 p.
- Roy, R. F., E. R. Decker, and D. D. Blackwell, 1968, Heat flow in the United States. *Journal Geophysics Res.*, v. 73, p. 5207-5221.
- Sass, J. H., W. H. Diment, A. H. Lachenbruch, B. V. Marshall, R. J. Munroe, T. H. Moses, and T. C. Urban, 1976, A new heat flow contour map of the conterminous United States: *U. S. Geological Survey open file report* 76-756, p. 24.
- Scholz, C. H., M. Barazangi, and M. L. Sbar, 1971, Late Cenozoic evolution of the Great Basin, western United States, as an ensialic interarc basin: *Geol. Soc. Amer. Bull.*, v. 82, p. 2979-2990.
- Shawe, D. R., 1972, Reconnaissance geology and mineral potential of Thomas, Keg, and Desert calderas, central Juab County, Utah: *U. S. Geological Survey Prof. Paper* 800-B, p. B67-B77.
- Shuey, R. T., 1974, Aeromagnetic map of Utah: Department of Geology and Geophysics, University of Utah and Utah Geological and Mineral Survey.
- Smith, T. B., 1974, Gravity study of the Fumarole Butte Area, Juab and Millard counties, Utah: M. S. thesis, University of Utah, 58 p.
- Smith, T. B., K. L. Cook, and W. J. Peeples, 1978, Gravity study of the Fumarole Butte area, Juab and Millard counties, Utah: *Utah Geology*, v. 5, no. 1, p. 37-56.

- Smith, R. L. and H. R. Shaw, 1975, Igneous-related geothermal systems: *in* Assessment of geothermal resources of the United States - 1975, D. E. White, and D. L. Williams, ed., U. S. Geological Survey Circular 726.
- Stewart, J. H., 1971, Basin and Range structure: A system of horsts and grabens produced by deep-seated extension: Geological Society of America Bulletin, v. 82, p. 1019-1044.
- Stokes, W. L., 1964, ed., Geologic map of Utah: Utah Geological and Mineral Survey.
- Stormer, J. C., 1975, A practical two-feldspar geothermometer: American Mineral., v. 60, p. 667-674.
- Stormer, J. C., 1972, Mineralogy and petrology of the Raton-Clayton Volcanic Field, north-eastern new Mexico: Geol. Soc. America Bulletin, v. 83, p. 3299-3322.
- Turley, C. T., and W. P. Nash, 1980, Petrology of late Tertiary and Quaternary Volcanism in Juab and Millard counties, Utah: This volume.
- Wender, L. E. and W. P. Nash, 1978, Chemical and mineralogical evolution of the Cenozoic volcanic rocks of the Marysvale area, Utah: Geol. Soc. Amer. Bull., Part II, v. 90, 34-76.
- Wones, D. R., 1972, Stability of biotite: a reply: America Mineral., v. 57, p. 316-317.
- Wones, D. R., and H. P. Eugster, 1965, Stability of biotite: Experiment, theory, and application: America Mineral., v. 50, p. 1228-1272.
- Wyllie, P. J., 1971, The dynamic earth: John Wiley and Son Inc., New York, 416 p.
- Wyllie, P. J., 1971, Role of water in magma generation and initiation of diapiric uprise in the mantle, Journal Geophysics Res., v. 76, no. 5, p. 1328-1338.
- Zielinski, R. A., P. W. Lipman, and H. T. Millard, 1977, Minor element abundances in obsidian, perlite, and felsite of calc-alkalic rhyolites: America. Mineral, v. 62, p. 426-437.

Appropriation No. 016103
Approval No. 8000068